Review

Role of Experimental, Modeling, and Simulation Studies of Plasma in Sustainable Green Energy

Muhammad Yousaf Arshad [1,2,*], Muhammad Azam Saeed [2], Muhammad Wasim Tahir [2], Ahsan Raza [3], Anam Suhail Ahmad [4], Fasiha Tahir [2], Bartłomiej Borkowski [5], Tadeusz Mączka [5] and Lukasz Niedzwiecki [6,7,*]

[1] Corporate Sustainability and Digital Chemical Management, Interloop Limited, Faisalabad 37630, Punjab, Pakistan
[2] Chemical Engineering Department, Lahore Campus, University of Engineering and Technology, Lahore 54890, Punjab, Pakistan; azam.saeed@uet.edu.pk (M.A.S.); wasim.tahir@uet.edu.pk (M.W.T.); fasiha.tahir59@gmail.com (F.T.)
[3] Aziz Fatimah Medical and Dental College, Faisalabad 38000, Punjab, Pakistan; ahsanra33@gmail.com
[4] Halliburton Worldwide, Sonora, TX 76950, USA; anam.ahmed@halliburton.com
[5] Institute of Power Systems Automation, ul. Wystawowa 1, 51-618 Wrocław, Poland; bartlomiej.borkowski@iase.wroc.pl (B.B.); tadeusz.maczka@iase.wroc.pl (T.M.)
[6] Department of Energy Conversion Engineering, Wrocław University of Science and Technology, Wyb. Wyspiańskiego 27, 50-370 Wrocław, Poland
[7] Energy Research Centre, Centre for Energy and Environmental Technologies, VŠB—Technical University of Ostrava, 17. Listopadu 2172/15, 708 00 Ostrava, Czech Republic
* Correspondence: yousaf.arshad96@yahoo.com (M.Y.A.); lukasz.niedzwiecki@pwr.edu.pl (L.N.)

Abstract: This comprehensive review paper offers a multifaceted examination of non-thermal plasma applications in addressing the complex challenge of tar removal within biomass-oriented technologies. It begins with a concise introduction to the research background, setting the context for our exploration. The research framework is then unveiled, providing a structured foundation for understanding the intricate dynamics of plasma–tar interactions. As we delve deeper into the subject, we elucidate the reactivity of tar compounds and the transformation of alkali metals through plasma-based methodologies, essential factors in enhancing product gas quality. Through an array of empirical studies, we investigated the nuanced interactions between plasma and diverse materials, yielding crucial insights into plasma kinetics, modeling techniques, and the optimization of plasma reactors and processes. Our critical review also underscores the indispensable role of kinetic modeling and simulation in advancing sustainable green energy technologies. By harnessing these analytical tools, researchers can elevate system efficiency, reduce emissions, and diversify the spectrum of available renewable energy sources. Furthermore, we delve into the intricate realm of modeling plasma behavior and its intricate interplay with various constituents, illuminating a path toward innovative plasma-driven solutions. This comprehensive review highlights the significance of holistic research efforts that encompass empirical investigations and intricate theoretical modeling, collectively advancing the frontiers of plasma-based technologies within the dynamic landscape of sustainable energy. The insights gained from this review contribute to the overall understanding of plasma technologies and their role in achieving a greener energy landscape.

Keywords: tars; kinetic modeling and simulation; non-thermal plasma; green energy; reactor performance

1. Introduction

Biomass is considered a viable and proven energy source, and it appears promising in terms of achieving carbon neutrality in the future [1–4]. In principle, biomass uses CO_2 from the atmosphere as a substrate during its growth [5,6]. Valorised biomass can be used in combination with fossil fuels, providing an opportunity for gradual replacement of the latter [7–9]. Moreover, the use of biomass in combination with CCS could result in

achieving negative emissions of CO_2 [10–13]. Gasification is a process capable of turning solid biomass into a mixture of combustible gases [14–16]. The gas from gasification, also called producer gas or syngas, could be combusted in an engine or turbine in order to produce electricity and heat. Moreover, such gas can be used as a substrate for chemical syntheses (thus the name syngas), including producing liquid fuels in the Fischer–Tropsch process [17]. Solid residues from gasification can be considered as biochar [18,19], and apart from applying to the soil, such porous carbon material [20] can also be used as a sorbent [21,22]. Furthermore, gasification using CO_2 is an interesting way of using captured CO_2 for energy purposes [23]. However, one of the most significant problems of gasification is related to byproducts of gasification—tars [24–26]. Tars are typically defined as a complex mixture of hydrocarbons with a molecular weight greater than the molecular weight of benzene [9]. Tars are deposited on cooler surfaces in many cases, significantly increasing the risk of fouling downstream process equipment. Thus, extensive research has been dedicated so far towards minimizing the production of tars during gasification, including in situ depletion at formation stage and its post gasification removal [27,28].

Plasma, an intriguing state of matter, offers tremendous potential for converting renewable energy sources into usable forms. One such application is the stabilization of ignition and extending the flammability limits [29,30], owing to both radicals as well as the thermal effect [31,32]. The non-thermal plasma can stabilize the combustion and even maintain the flame for an equivalence ratio of 0.95 [33]. Moreover, the propagation of a turbulent flame can be enhanced by using nanosecond repetitively pulsed plasma discharges [34]. The thermal effect is extremely important at the scale of a power plant boiler, as reported by Messerle et al. [35]. The minimum attainable power of solid fuel-fired power plant boilers can be significantly reduced by the use of plasma technologies [36]. Over 27 boilers in Kazakhstan, Ukraine, Mongolia, China, and South Korea have been used in successful trials of using plasma torches to support combustion [37]. A suite of tests performed on BKZ-420 power boiler (Almaty Power Plant, Kazakhstan) proved a successful startup operation using only a system of plasma torches without using heavy oil as a supplementary fuel [38]. The trials were carried out using Ekibastuz coal with a high ash content (40% when dry) and a low calorific value (16.6 MJ/kg). The combustion of pulverized coal with a relatively low volatile matter content could be sustained, with the power of plasma torches being 2.5% of the burner's power, according to Karpenko et al. [37]. The economic feasibility of such solutions has been proven by Mączka et al. [34]. The application of non-thermal plasma has also been considered as a way to abate the emissions in the energy sector and is readily being used in formulation of bio-based feedstocks for energy utilization rather than material transformation to supplementary chemicals and bio-composites [39–41].

Another environmentally friendly application of plasma technologies can be found in the field of gasification [42,43]. Plasma gasification has been successfully used for the gasification of organic waste [44], spent lubricants [45], or refuse-derived fuel [46]. An important advantage of plasma gasification with respect to different types of waste is its ability to perform vitrification [47]. The use of plasma for modification of the surface of different materials [48], including hydrochars, has also been reported [49–53]. Some authors also reported the use of plasma for the degradation of organic pollutants [54].

Looking at the Scopus database, significant growth in papers published annually with keywords such as plasma and modeling can be noted in recent years (see Figure 1) due to increased interest in plasma processes. There are existing reviews on plasma processes as well as on their modeling, including works on process modeling for the synthesis of chemicals [55–57] and plasma gasification [58]. However, there is a lack of reviews on the modeling of non-thermal plasma for the decomposition of tars, which is one of the key applications of plasma processes in the sustainable green energy sector.
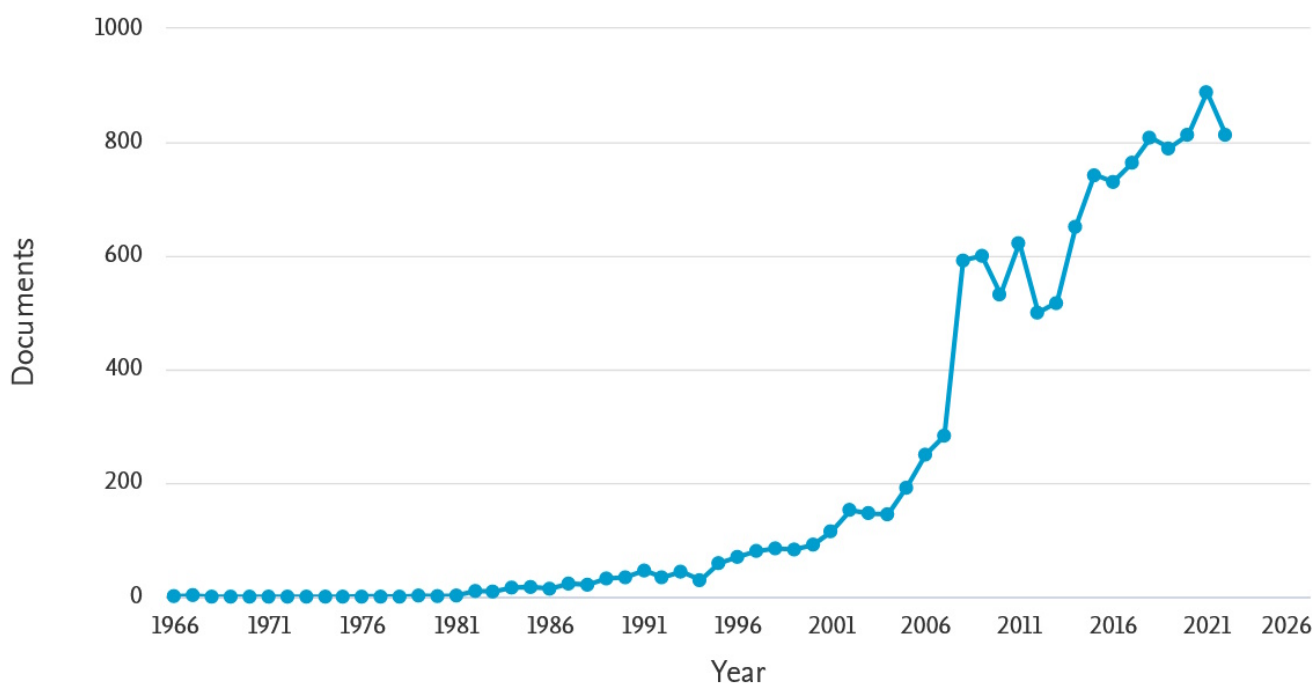
Figure 1. Number of papers published each year between 1966 and 2022 with keywords plasma AND modeling, shown by Scopus.

This review aims to close this gap by exploring the wide range of applications of plasma-based technologies in sustainable green energy, with a specific focus on the modeling of non-thermal plasma decomposition of tars. These technologies not only provide eco-friendly solutions for waste disposal but also generate clean energy, making them vital components of a sustainable energy landscape [41,51,59]. One significant challenge in biomass-oriented technologies is the efficient removal of tar, a complex byproduct of gasification. Understanding the reactivity of tar and the transformation of alkali metals using plasma technologies is crucial for enhancing the quality of product gas and advancing the commercialization of biomass processes [41,59]. Experimental studies investigating the interactions between plasma and various materials yield valuable insights into plasma kinetics, modeling, and the optimization of plasma reactors and processes [53,60]. Moreover, understanding novel environmentally friendly technologies is important from the point of view of regulatory bodies, as effective environmental regulation tools can strengthen the stakeholder relationship between the government and enterprises and thus create the right environment for the implementation of green technological innovation [61]. Stable policies are key since changes between economic cycles influence energy intensity, especially in emerging economies, which in turn influences the adoption of eco-innovative technologies by industrial stakeholders [62].

This review emphasizes the pivotal role of kinetic modeling and simulation techniques in contributing to sustainable green energy technologies. By employing these tools, researchers can improve system efficiency, reduce emissions, and expand the utilization of renewable energy sources. Modeling plasma behavior and its interactions with different components facilitates the development of innovative plasma-based solutions [52].

This paper provides a comprehensive overview of the key subtopics in plasma-based technologies for sustainable green energy. It covers areas such as tar characteristics in gasification processes, mechanisms and reactivity of tar cracking and reforming through thermal, catalytic, and plasma-assisted decomposition, plasma modeling and chemical kinetic modeling for understanding plasma processes, and the relationship between reactor geometry, energy yield, and mass transfer in plasma reactors.

Furthermore, it explores the simplification of removal kinetics modeling through direct electron collision and its relation to reactor configuration and scaling-up studies. The use

of lumped parameters and kinetic models for tar removal in synthetic gas mixtures using a pulsed corona discharge reactor is also discussed, along with the thermodynamics in kinetic models for tar removal considering moisture content and equivalent ratio. The development and validation of kinetic models for hydrocarbon conversion in non-thermal plasma reactors, the role of energy density and efficiency in plasma discharge kinetics modeling for decomposition reactions, and the application of kinetic modeling for tar decomposition in plasma reactors with varying energy density and carrier gases are examined. The efficiency of tar removal in pulse discharge reactors using NIST-based kinetic modeling and numerical simulation, as well as the effect of temperature and gas composition on tar removal efficiency in non-thermal plasma and pulsed corona discharge reactors using kinetic modeling and statistical analysis, are also addressed.

This comprehensive review consolidates the current knowledge on plasma-based technologies for sustainable green energy. The insights gained from this review contribute to the overall understanding of plasma technologies and their role in achieving a greener energy landscape. By harnessing the unique properties of plasma, we can pave the way for a more sustainable and environmentally friendly future for biomass-based green energy.

2. Characteristics of Tar in Gasification Processes: Classification, Reactivity, Composition, and Environmental Impact

Different classifications of tars exist, with the most common being the ECN classification. According to this classification all tars undetectable by GC (heaviest tars) belong to class 1, heterocyclic compounds (e.g., phenol, pyridine, and cresol) belong to class 2, aromatic compounds with one ring (e.g., xylene, styrene, and toluene) belong to class 3, light polyaromatic hydrocarbons with 2–3 rings (e.g., naphthalene, biphenyl, acenaphtylene, phenanthrene, and anthracene) belong to class 4, whereas heavy polyaromatic hydrocarbons with more than three rings (e.g., fluoranthene, pyrene, and chrysene) belong to class 5 [63]. Some of the recent works suggested classifying tars depending on the melting point of each compound, thus enabling the possibility of making a tar deposition diagram (Figure 2), which is a useful tool for quantitative prediction of tar deposition issues downstream of a gasifier.

Tar can be polar or non-polar, reactive or unreactive, and hydrophobic or hydrophilic based on temperature variation in the gasifier and feedstock. Feedstock degradation has a temperature range of about 300–400 °C, and it forms water vapor. Primary, vapor formation has a higher tar yield with an increase in temperature during cracking increases. At temperatures higher than 800 °C, poly-aromatic hydrocarbons yield higher tar [64]. A thermochemical conversion of combustible gases at temperatures 800–1000 °C in an air/oxygen mixture usually leads to partial oxidation reactions, typical for gasification. A mixture of steam/oxygen can be considered auto-thermal depending on the equivalence ratio and ratio of oxygen to steam. Producer gas composition depends on the gasifying agent (O_2, steam, etc.) and gasifier configuration, i.e., if it is a fluidized bed, fixed bed, or entrained flow gasifier [63,65]. Figure 3 provides a representation of the diverse product composition in different types of gasifiers, highlighting the importance of understanding the variations in gasifier performance and product yields.
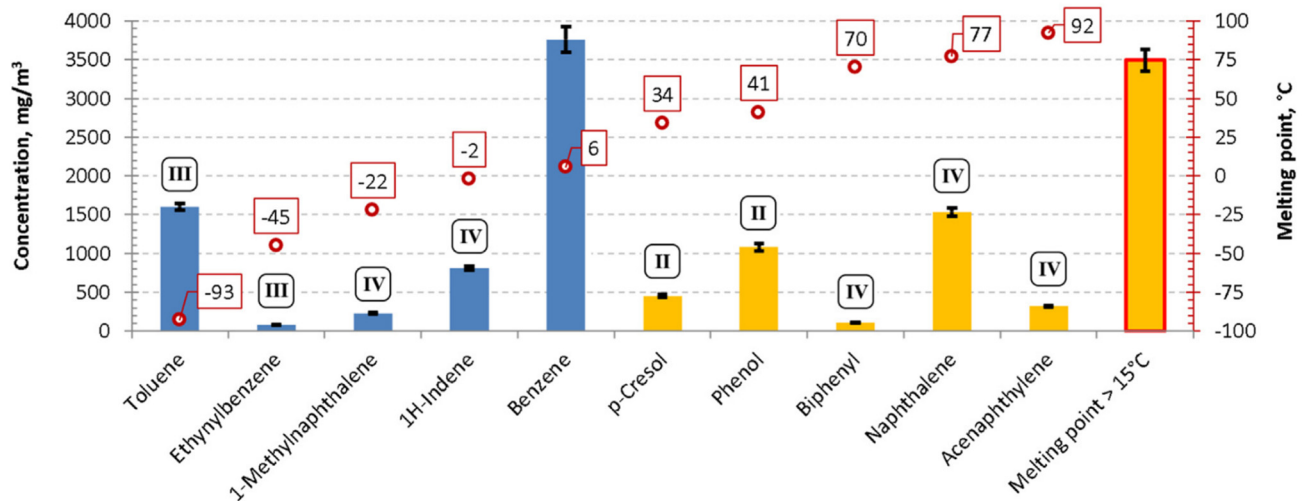
Figure 2. An example of the tar deposition diagram for a fixed bed gasifier with a simple gas cooler with an inlet water temperature of 15 °C (Roman numerals indicate the class of the particular compound, based on the ECN classification)—reprinted from [66] with permission from Elsevier.
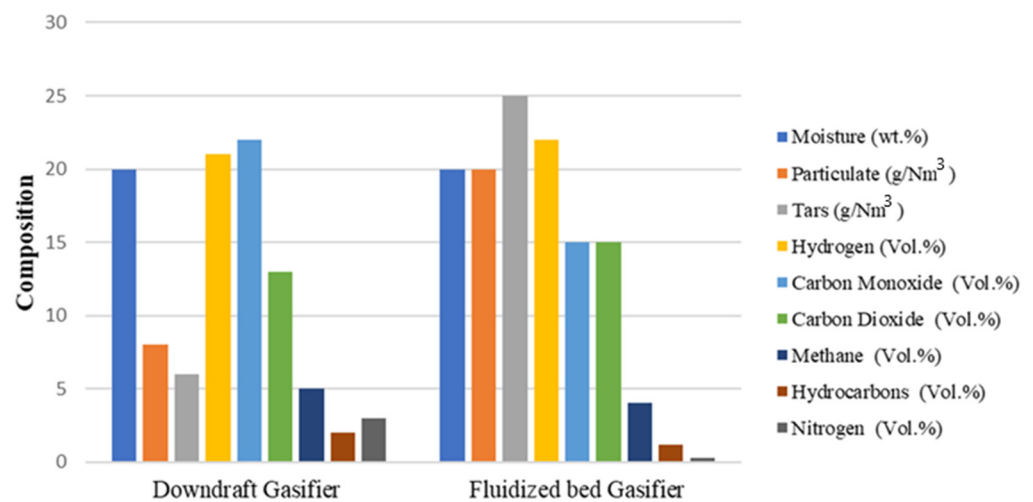

Figure 3. Different types of gasifier product composition—based on [67].

Scientific research activities are being conducted extensively to enhance the understanding towards tar removal. Tar is used in any form of gasification process except in boiler operations. Tar is one of the reasons for particulate matter formation at downstream operations. The content and composition of produced tars depend on the design of a particular gasifier, e.g., a typical downdraft fixed gasifier produces a tar within the range of 500 g/cm^3 to 1000 g/cm^3. Municipal waste is another source of energy production through gasification and also produces a good quantity of syngas. The process produces enough activity for an environmental impact and reduces waste deposits in landfills [64,68]. Moreover, many compounds contend among tars, are considered pollutants [69] and are subject to control, as shown in Figure 4, which illustrates the maximum permissible limits of emissive pollutants. From this perspective, any leaks from gasification installations could increase concentrations of the mentioned pollutants in the atmosphere.

Tar reactivity research is the core step for the development and commercialization of biomass-oriented technologies as it initially removes tar and increases producer gas quality. For the commercialization of a gasification-based energy stream, a two-way methodology is proposed, initially by parametrically optimizing gasifier operations through tar removal using primary and secondary methods [63,70]. Primary methods are not absolutely efficient for gas cleaning downstream but are comparatively economical. Process parameters, i.e.,

temperature, equivalence ratio, compositions, reactor residence time, pressure, etc., are vital for enhanced tar reduction and syngas quality. The primary tar removal method might decrease the chemical energy and overall system efficiency [65,71–73]. Figure 5 illustrates the different commercial primary and secondary tar removal methods used in the industry.
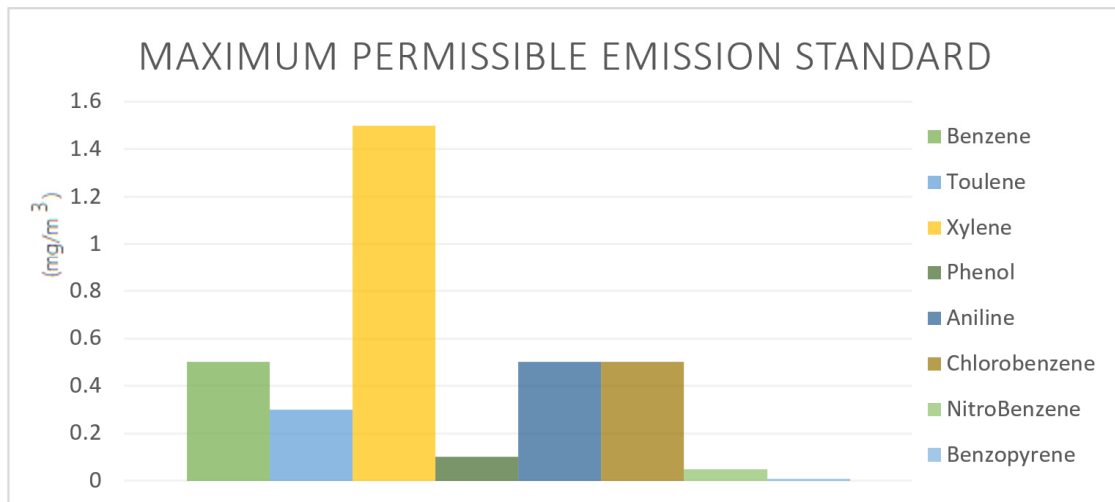

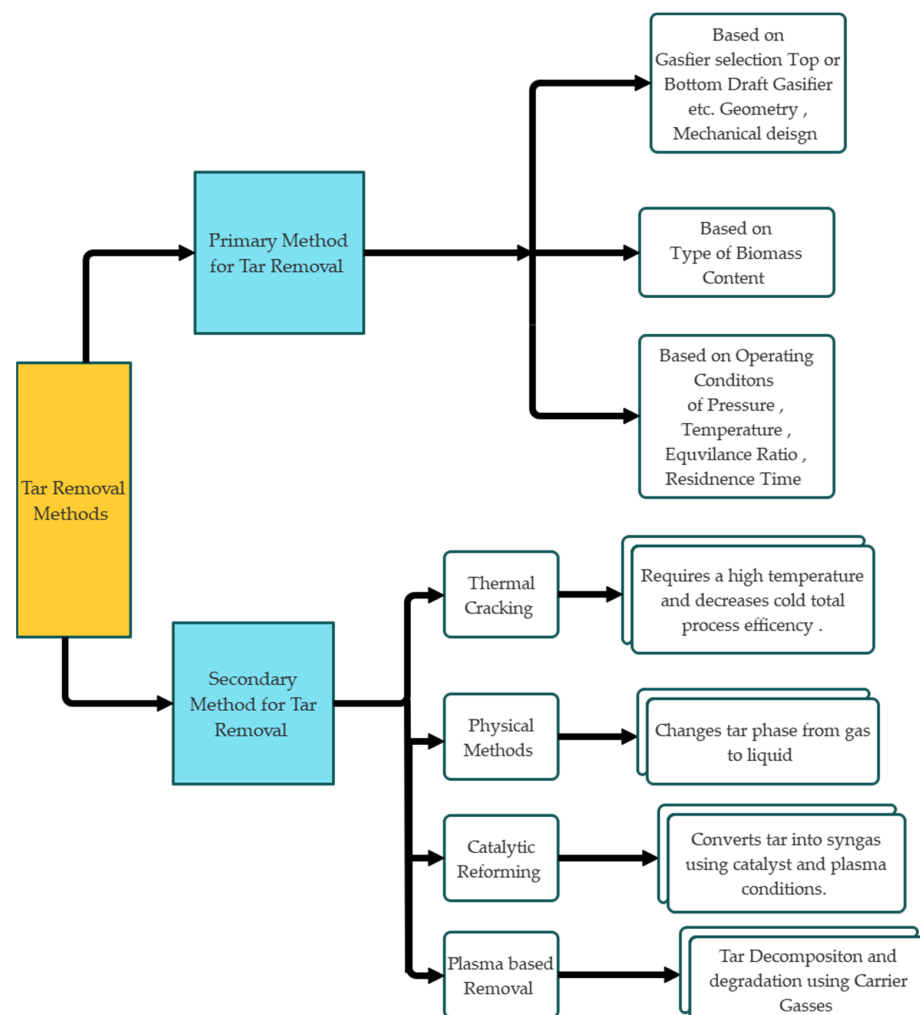**Figure 4.** Maximum permissible limits of emissive pollutants—based on [69].

Figure 5. Commercial tar removal primary and secondary methods for tar removal—based on [63,70].
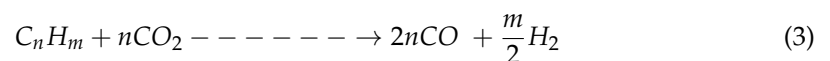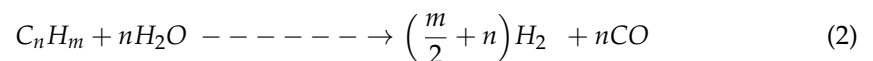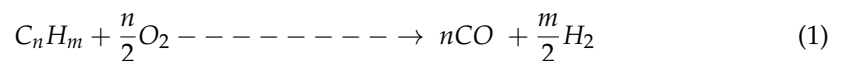
3. Tar Decomposition Mechanisms and Kinetics in Thermal and Plasma Environments

Plasma-based technologies hold immense potential in converting renewable energy sources into usable forms and play a critical role in sustainable green energy applications. The focus on plasma combustion and plasma gasification offers eco-friendly waste disposal solutions and clean energy generation, making them integral to a sustainable energy landscape. The removal of tar using plasma technologies is a key area of interest, requiring a deeper understanding of tar reactivity and the transformation of alkali metals. Experimental studies on plasma–material interactions provide valuable insights into the kinetics, modeling, and optimization of plasma reactors and processes.

The decomposition of tar and its constituent compound family using conventional thermal, catalytic, and advanced plasma routes allows a further in-depth understanding of tar reactivity. At elevated temperatures, tar undergoes a series of reactions with definite residence time at ambient conditions and exposure to air. Mainly, the reactions are symmetric and categorized as tar polymerization and tar decomposition. Initial reactions are decomposition reactions, while intermediate stages are polymerization reactions which feature condensed tar reactions and inert environment tar decomposition between heterogeneous (liquid and gaseous phase) compounds and subsequent char or ash. Final reactions occur between gaseous species and tar compounds. The rate of radical formation determines cracking reactions and is dependent on the size, number, and least bond strength of the model compound in thermal and non-thermal settings [63,74,75].

Tar cracking is divided into four categories, partial oxidation, steam reforming, dry reforming, and hydrocracking and thermal cracking, which are mainly dependent on temperature, an increase in process temperature, and a change or sudden decrease in the activation energy. Plasma cracking and reforming complement the above two in the most sophisticated manner using a catalyst [64]. In catalytic cracking, fragmentation and carbon deposition decreases operational cost [76]. Kai studied an efficient route of plasma catalytic reforming for tar conversion into syngas and superior gas cleaning activity simultaneously. Toluene, being a model compound, decomposes in Ni/SiO_2 catalyst for syngas production. According to Wnukowski and Moroń, the conversion of toluene in a microwave plasma generates heavy aromatic by-products, such as phenylethyne, indene, naphthalene, and acenaphthylene [26]. Moreover, tar removal from a real producer gas has also been attempted using microwave atmospheric plasma [77].

A comparison between thermally induced direct decomposition and plasma-supported decomposition shows that plasma induction just before catalyst beds increases the conversion rate towards syngas formation. A comparison of the aforementioned methods with catalytic reforming and plasma-assisted decomposition shows that plasma catalytic reforming shows the conversion rate is the maximum and the direct decomposition rate is the minimum. The sequence is as follows: plasma enhanced reforming > plasma decomposition > catalytic reforming > direct decomposition [78,79]. The tar reforming mechanism is depicted in Figure 6, and reactions are shown in Equations (1)–(3) [64,65,80].

$$C_nH_m + \frac{n}{2}O_2 - - - - - - - - \rightarrow nCO + \frac{m}{2}H_2 \tag{1}$$

$$C_nH_m + nH_2O - - - - - - \rightarrow \left(\frac{m}{2} + n\right)H_2 + nCO \tag{2}$$

$$C_nH_m + nCO_2 - - - - - - \rightarrow 2nCO + \frac{m}{2}H_2 \tag{3}$$

Close relationships between gasification reactor parameters give rise to in situ strategies that are usually complex in nature. An increase in gasification temperature decreases the yield of gasifier tar with a change in gas composition. An increase in gasification rate could be achieved by an increase in the temperature. Equilibrium reactions and reduction in available tar are affected by gasifier operational parameters. This limits the first gasification stages to maximize the conversion of total carbon and minimize tar reduction in the

second stage. The required process should not only decrease tar contents but also provide higher syngas quality, with minimum by-products and an increase in the dew point and soot formation. A plasma gasifier takes its heat content from auto-thermal reaction and oxidation processes. The high temperature in plasma gasifiers destroys toxic and dangerous molecules. Thermal plasma units are also used as secondary treatment units. Usually, in hot gas thermal plasma, gas is heated instead of the feedstock. It reduces tar and carbon soot but is extensively heat-dependent [64,81,82].
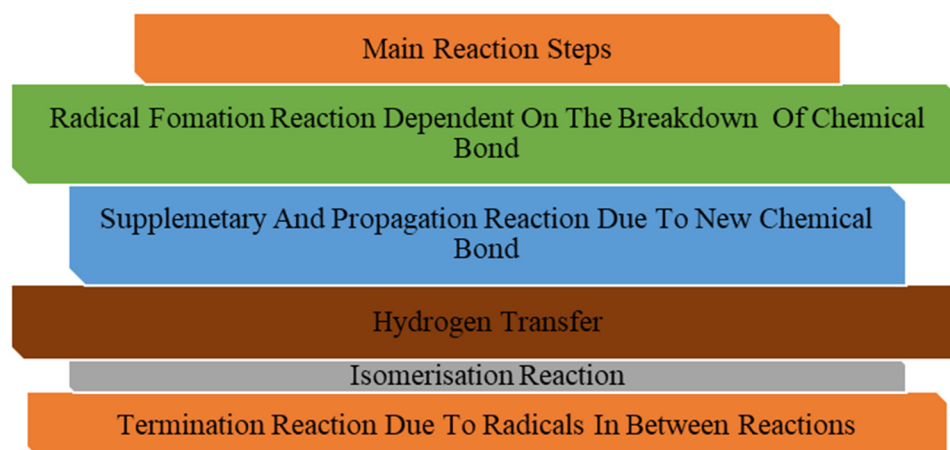

Figure 6. Tar Reforming Reaction Mechanism main steps.

Tar model compounds naphthalene, toluene, and benzene are thermally converted in the presence of hydrogen and steam to understand the mechanism and kinetics of the reaction as a function of temperature in a definite time function of 0.5 s. The order to reactivity is toluene > naphthalene > benzene as the activation energy of benzene is highest while toluene has lowest. The activation energy of toluene, naphthalene, and benzene are 247.1 kJ/mol, 350.2 kJ/mol, and 443.6 kJ/mol, respectively [72]. In thermal decomposition, mainly benzene is produced. Benzene has the highest activation energy, along with soot and aromatic hydrocarbons, as a principal compound from higher hydrocarbon molecules such as naphthalene. The reduction method should not incorporate an effect on gaseous products such as CO, H_2, CH_4, and CO_2 [63,80,83,84]. In the research of Nair [51], the author constituted the utilization of pulse discharge for the removal and cleaning of product gas for industrial applications. Experiment conditions were 200 °C for heavy hydrocarbon in an oxidation reaction process [51]. In pulse corona discharges, an energy transfer from the power source to the gaseous mixture is initiated for radical production, which defines efficiency. Streamer corona discharges are relative to reaction rates and termination reactions for achieving a removal efficiency of 90% [85–87]. Tar composition is mainly dependent on the varying equilibrium conditions in different gasifiers. On the other hand, combustion reactions are at equilibrium and do not produce tars [40].

4. Plasma Chemical Kinetic Modeling: Relationship of Reactor Geometry, Energy Yield, and Mass Transfer in Plasma Reactor for Hydrocarbons and Volatile Organic Carbon Conversion

Kinetic modeling and simulation techniques play a pivotal role in advancing sustainable green energy technologies. By utilizing these tools, researchers can enhance system efficiency, reduce emissions, and expand the range of renewable energy sources available for use. Comprehensive research efforts, encompassing both experimental investigations and theoretical modeling, are necessary to drive the development of innovative plasma-based solutions. Plasma modeling is a helpful method for understanding the plasma process and building a chemical kinetic model for predicting key reaction data, i.e., rate constant, conversion, and cross-section [88]. Usual plasma process modeling problems initially have the flow of carrier/background gas, breakdown, and transport existing in

the field of fluid dynamics. The creation and subsequent destruction exist in the realm of plasma chemistry, and chain reactions within species are kinetic modeling. Chemical species integration decomposition ensures the behavior of process development according to operating conditions and analytical models such as zero-dimensional reaction kinetics chemical model (0-D) and simulation. Kinetic modeling and simulations are simplified with either diffusion consideration in special cases or only computation of reaction rates in general. Diffusion terms often consider atomistic calculations [89]. A detailed consideration for ion-to-neutral species shows an effective channeling for the removal process within a strong electric field. Comparison between two approaches for modeling tar removal ion-molecule infinite fast reactions is used for G-value calculations. The secondary approach designates a kinetic based on ions and electrons. G-value based on the primary approach of ion–neural interaction is more comparable [27,28]. The study incorporates Figure 7, which demonstrates the NTP plasma decomposition and microscopic kinetic timeline of the complex reaction pathways involved in tar decomposition.

For a range of up to 240 mm benzene initial concentration, a silent discharge plasma reactor has been investigated. The relationship has been developed for understanding reactor geometry, energy yield, and rate of conversion in benzene with quartz-type material inner electrode and varying diameter. An additional parameter, space velocity, has also been studied. At optimum conditions, an energy yield of 255 J/L, space velocity of 188.1 h^{-1} at 60% conversion rate with 6 mm and 1333 quartz and bolt type electrodes for applied high voltage. Destruction of benzene has been identified in GC-Ms, which shows pentanoic acid, phenol, hydroquinone, and 4-phenoxy phenol is obtained. Destruction of benzene in NTP is usually very complex in reaction nature. The products usually formed are CO_2, CO, and H_2O with electron and radical impact dissociation. The two paths, i.e., electron impact or radicals-based dissociation, play an active role in destruction or decomposition [90]. In NTP reactors, in addition to kinetic modeling, mass transfer is an important feature. Mass transfer and kinetic reactor rates are synergistically effective for novel continuous reactions and show a greater selectivity of heavy hydrocarbon and volatile organic carbons, such as benzene and naphthalene, using photocatalysis. The hybrid modeling approach allows an agreement between kinetic modeling and empirical results of the mass transfer of complex nature in plasma reactions. Synergistic effects and hybrid models allow a simulation of NTP with photocatalysis without knowing the reaction's plausible pathways and kinetics in-depth with information on mass transfer in relation to total modeling terms [91].
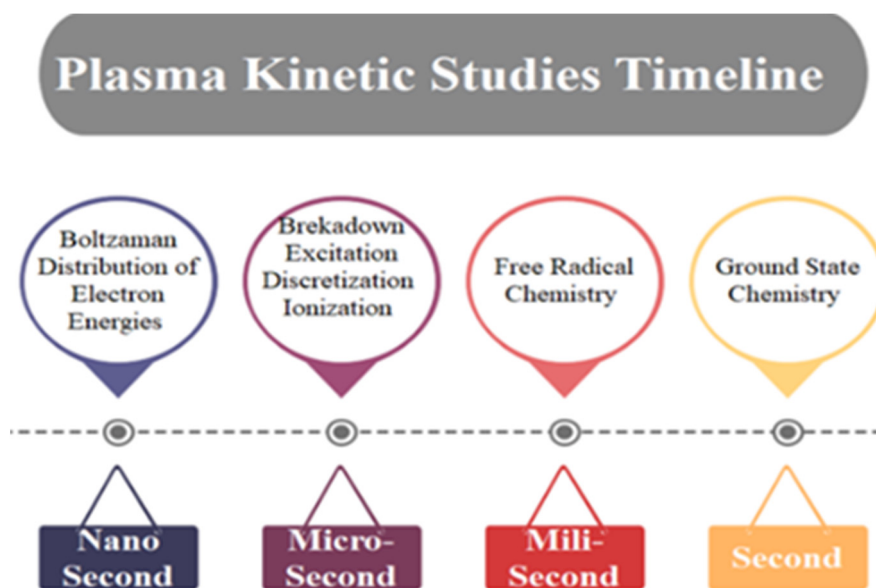

Figure 7. NTP plasma decomposition and microscopic kinetic timeline—based on [90,92].

Plasma discharges are divided mainly into two modes: homogeneous and streamer discharge mode. In plasma modeling, we can include a 1-D or 2-D streamer model for discharge propagation. The phases of modeling are segmented into an avalanche, streamer/discharge, and finally, decay phase. The barrier is also affected by the frequent streamer or discharges, and its surface starts to lose charges. This eventually increases the applied voltage. Factors such as frequency, gas temperature, electrode length, and applied voltage govern the decay and degeneration of metastable species required for the determination of discharge modes [74,93].

5. Energy-Efficient Removal Kinetics Modeling in Plasma: Investigating Direct Electron Collision and Its Impact on Reactor Configuration and Scaling Up Studies

The energy-efficient removal kinetics modeling in plasma has focused on the direct electron collision with compounds, neglecting the pulse discharge rate. The destruction reactions in plasma are based on C–H bond breakage, leading to the formation of various byproducts. The kinetics of plasma reactors are influenced by reactor configuration, scaling-up studies, reactor hydrodynamics, and spatial and temporal studies. Figure 8 illustrates the step-by-step NTP reactor parameters used for kinetic plasma modeling in the study. In plasma, removal kinetics modeling has been a difficult task owing to the absence of data within intermediate conditions. To simplify, the kinetics of direct electron collision with a compound has been studied, neglecting the pulse discharge rate. Total destruction reaction is based on C–H bond breakage, which initially leads to phenyl due to hydrogen abstraction. The energetic electron's reaction by products of radicals and phenyl. Intermediates upon being attacked by electrons convert to CO, CO_2, and finally, the aromatic structure breaks down. Nitrogen bonds are of a peculiar nature and energetic electrons in direct dissociation due to high bond energy usually form nitro-alcohols from NO_2 faster with nitrogen and oxygen radical reactions [27,94]. Figure 9 illustrates the step-by-step process of tar removal in a plasma reactor, providing a visual representation of the mechanisms and stages involved in the efficient elimination of tar.
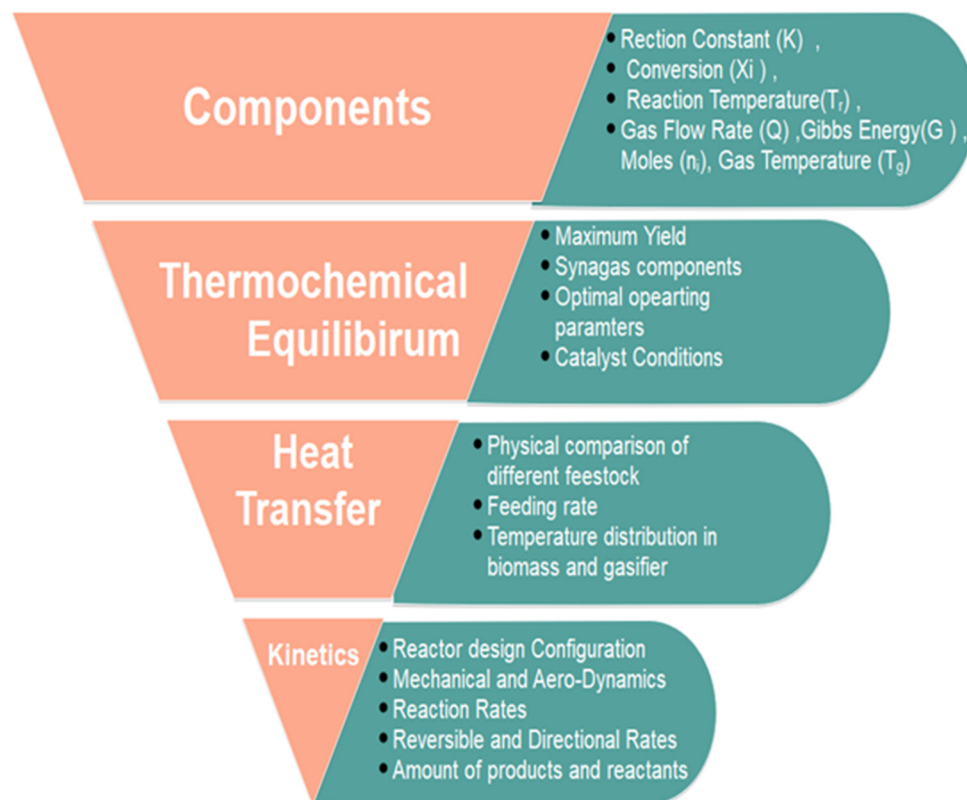

Figure 8. NTP reactor parameters for kinetic plasma modeling step by step—based on [74].

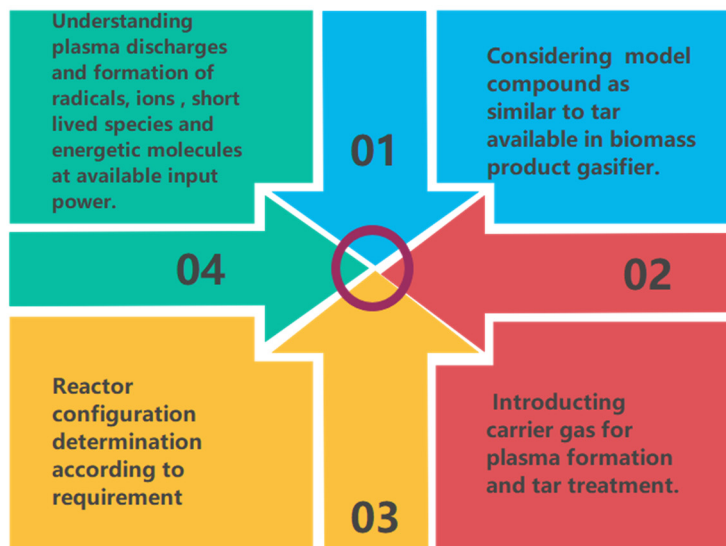# Novel Combinations for Understaing Tar Removal in Plasma Reactors

Figure 9. Step by step understanding of tar removal in plasma reactor—based on [94].

Most modeling studies are based on inlet feed parameters such as temperature, pressure, molar flow rate etc., along with plasma factors such as frequency, electrode gap and configuration, applied external current to voltage ratio, and catalyst bed length and types. In the literature, two significant reasons are defined for kinetic studies of plasma reactors:

- Change in reactor configuration and complicated upscaling of modular reactor design.
- The non-equilibrium nature of plasma intrinsically involves spatial and temporal studies complimenting the reaction rates for species conversion and decomposition.

Table 1 provides valuable insights into the chemical reaction kinetics parameters for different kinds of plasma reactors. In chemical reaction engineering, scale-up studies are based on different parameters. Reactor hydrodynamics is a significant factor in understanding fluid regimes for laminar and turbulence flow and its relationship with plasma reactor performance. A hypothesis has been decided for the synergizing of a plasma packed bed reactor equivalent to plug flow reactor. Mainly, selectivity, energy efficiency, and conversion are important factors for scale-up studies in plasma reaction engineering [73,95].

Table 1. Chemical reaction kinetics parameters for different kind of plasma reactors [73].

Reactor Type	Batch Reactor	CSTR Reactor	PFR Reactor
Generalized Equation	$\frac{Ca}{Co} = \exp(-kt)$	$\frac{Ca}{Ca\ in} = 1(1 + k\mathrm{T})$	$\frac{Ca}{Ca\ in} = \exp(-k\mathrm{T})$
Space Time	$t = \frac{V}{Q}$	$\mathrm{T} = \frac{V}{Q}$	$\mathrm{T} = \frac{V}{Q}$
Conversion X, n = 1	Conversion is greater than CSTR for first order reaction	Conversion is less for first order reaction than PFR	Conversion is greater for first order reaction
Reactant Density p	Usually, fluid density is kept constant	Usually, fluid density is kept constant	Usually, fluid density is kept constant
Variable Order of Reaction	Conversion is greater than CSTR if n > 0, T= *constant*	Conversion is less than PFR if n < 0, T= *constant*	Conversion is greater than CSTR if n > 0, T= *constant*
At n = 0	Conversion is the same as another reactor	Conversion is the same as another reactor	Conversion is the same as another reactor

In the literature, tar removal studies usually consider tar as a lump and, mainly, three compounds are used as analogues, i.e., toluene, benzene, and naphthalene. These compounds are mainly primary, secondary, and tertiary representatives of tar. The mechanism and chemical kinetics are usually neglected in lump parameter modeling. Hundreds of detailed chemical reactions make the models complex within modeling, so for the practical approach, we usually designate minimum representative compounds and reactions. The lumped model usually considers the deposition reaction. Usually, three kinds of kinetic models are studied in the literature.

- Single model approach;
- Lumped model;
- Detailed kinetic model approach.

The kinetic equation is fitted with respect to experimental data. A significant drawback of lumped models lies in the process due to heavy hydrocarbon involvement that is sensitive to temperature and minimum concentration, which allows condensation [91,96]. A pulsed corona discharge reactor at 200 °C is subjected to tar removal in the synthetic gas mixture. Tar removal is subjected to an oxidation process mainly due to CO molecules. The literature recommends three-way reaction models for the removal of corona discharge in tar removal, which is dependent on the radical generation that corresponds to total energy efficiency. Figure 10 illustrates the kinetic modeling nexus, showcasing the relationship between linear and non-linear data sets for reactor performance. Three types of chemical kinetics models are defined for the non-thermal plasma reactor [87,97].
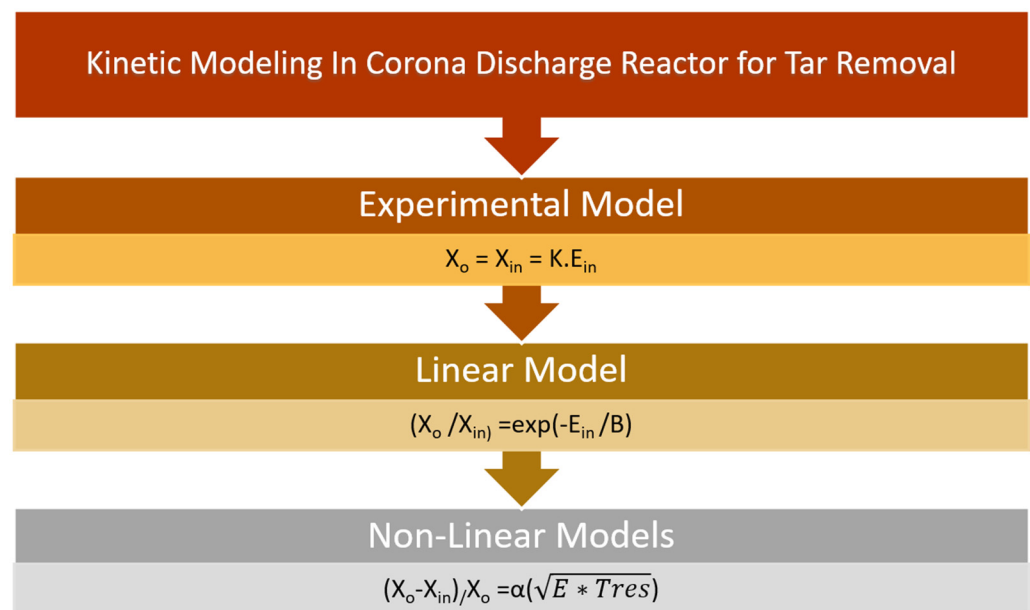

Figure 10. Kinetic modeling nexus with linear and non-linear data-set for reactor performance—based on [87].

5.1. Zero Effect Radical Termination Kinetics Model

It has a parallel and in-series combination and usually has a similar processing efficiency for pollutant removal. The energy yield in the overall reactor is a constant sum. The G-value is not a function of temperature. An increase or decrease in residence time does not change radical termination, while the energy density is the measure of the removal efficiency of a reactor. This zero-effect kinetic model and combination are the most effective nature as compared to the other two.

$$X_0 - X = \alpha \cdot E \qquad (4)$$

5.2. Reasonable Linear Radical Termination Kinetics Model

It has a parallel and in-series combination, and an increase in reactor number usually has a similar processing efficiency for pollutant removal as compared to two reactor configurations. Energy yield has an inversely proportional relationship with the energy density. G-value is a good function of temperature. An increase and decrease in residence time does not change radical termination, while the energy density is the measurement of the removal efficiency of a reactor. The linear kinetic model and combination in hybrid, i.e., series and parallel, is of considerable nature for removal efficiency comparison.

$$\frac{X_0}{X} = \exp\left(-\frac{E}{\beta}\right) \tag{5}$$

5.3. Non-Linear Radical Termination Kinetics Model

It has a parallel and in-series combination, and an increase in reactor number increases processing efficiency with due repeated treatment total removal efficiency. Energy yield has an inversely proportional relationship with the energy density. G-value is a good function of gas temperature and time, so it increases proportionally with both variables. Removal efficiency of pollutants is a dependent function of energy density along the time frame but lacks the linear radical counterpart model. Hybrid combination, i.e., series and parallel, is of considerable nature for increasing removal efficiency comparison.

$$(X_o - X_{\text{in}})/X_o = \alpha\left(\sqrt{E * Tres}\right) \tag{6}$$

Energy requirements can be minimized by reaction conditions that are needed where the kinetics for tar removal are more advantageous as compared to termination reactions. To achieve this, insight into the chemical processes involved is necessary. This can be obtained by determining the energy needed for tar removal at various gas mixtures. In order to establish relative trends in energy requirement with respect to different radicals, NTP reactors require minimum energy inputs for the establishment of optimum reaction conditions based on the radical propagations and termination reactions [98]. The harmony of experimental and modeling results shows that incorporating the corona discharge reactor for tar removal is optimally possible at 200 °C. Studies show that mainly tar in corona discharge occurs due to CO_2 dissociation. Energy intakes increase due to the background CO radical termination. Mainly, the oxidation of naphthalene reactions is analogous to NTP reactor breakdown of model compounds in terms of byproducts. Carrier gases such as hydrogen, methane, and moisture content do not increase the destruction rate or energy efficiency [99,100]. Cold plasma reactors and atmospheric reactors utilize perforated dielectric electrodes embedded in low-field electric fields for corona discharges. Negative polarization of the electrode gains the highest energy yield of 2.5 g/kWh for toluene [101]. Pressure conditions have an effect on negative corona discharge. The N_2, He, and air plasma discharge decreases with increases in pressure. At 10 MPa with an electrode gap constant at 10 mm, the breakdown is lower than 2 MPa. The model produces a quadratic formula for I-V and hysteresis due to an increase in temperature and pressure. Such an increase in removal and decomposition phenomena only complements the spark over corona discharge. Aspen software V14 uses an equilibrium-based model for the chemical composition of producer gas in the property estimation for thermodynamic conditioning. Hydrodynamic and reaction kinetics are also being studied for fluidized gasifiers at atmospheric conditions. Equilibrium studies in Aspen software have been carried out to understand the chemical composition and heating values of the biomass waste-based syngas produced. The yield of char and tar in the gasification process has been carried out in Aspen for methanation and water gas shift reaction studies, and experimentation and simulation results for 16 samples were compared [98].

6. Thermodynamics in Kinetic Models for Tar Removal in Moisture Content and Equivalent Ratio

The study on thermodynamics and kinetic models for tar removal in moisture content and equivalent ratio in non-thermal plasma (NTP) discharge reactors has provided valuable insights into the behavior of different biomass under various gasification conditions. Humidity, as an important parameter, impacts the electronegative process, coating, and dielectric materials in the reactor. Humidity is not only a parameter for physical studies but also for chemical studies. The OH^{-1} is short-lived, so sometimes its role in decomposition and humidity factor is neglected [102]. The thermodynamic model has been proposed for ER and MC conditions.

$$ER = 0.008 \times MC + 0.174 \qquad (7)$$

As the MC increases, a more equivalent ratio is required as the moisture vaporization requires a higher temperature. An increase in the moisture content, reaching 40%, decreases the energy lower heating value by 1.13 MJ/m_N^3. The average error difference between experimentation and simulation is 15% in available combustible gases in the syngas mixture, and a lower heating value (LHV) of 7% in simulation has been proposed [103]. The study of chemical kinetics is for reactor design and for commercialization of tar removal process and feasible process. Reaction kinetics signifies the reaction associated with the formation of products [104]. Chemical kinetics studies of heavy hydrocarbons and active species in plasma (mainly radicals, excited species, and ions) have not been studied extensively. A self-sustained kinetic model for the plasma reactor of corona discharge has been used to compare the cleaning of producer gas from naphthalene in discharge and post-discharge environments [27,105]. In the DBD reactor, a toluene destruction behavior has been studied at atmospheric conditions [106]. The anomalous interaction of electrons with excited oxygen atoms breaks the model compound ring. In detail, mechanism studies of toluene breakdown in chromatography have been restricted due to the quenching effect of N2A3∑. In toluene, removal of the electric field E/N effects temperature lesser than electron density n_e. The results indicate that in O_2, N_2, and in air during a plasma pulse reactor a greater possibility of chlorinated intimidates are possible leads to dichlorination reaction and accounts for 78.5%, 50%, and 12.5% removal efficiency during dichlorination reaction [106].

The AC/DC corona system has been an efficient tool for tar and NO_x removal. Toluene and benzene are subjected to linear radical removal (Figure 11). Styrene procures a greater amount of aerosol and oxygen-containing compounds such as carboxylic groups -COOH, -OH when examined on the FITR studies. Wang proposes a global kinetic model on experimentation data and deduces an order for degradation reaction. Experiments were carried out with individual compounds in the air. Corona-specific energy density calculated by experimentation is totally different for the removal processes of three benzene derivatives. Benzene and toluene were significantly dominated by linear radical termination reactions as compared to styrene. A mathematical model equation for benzene derivatives kinetics degradation reactions is:

$$\frac{C(t)}{C_o} = \exp\left(\frac{-\varepsilon}{\beta}\right) \qquad (8)$$

$C(t)$ is the final concertation, C_o is the initial concentration, β is the energy constant, and ε is the specific energy density. Calculated energy constants are given in Table 2. Furthermore, Table 2 provides valuable insights into the energy yield and beta value of various plasmas for different species in different plasma plate plasma reactors. Benzene, 1-methylnaphtalene, and toluene are decomposed in the microwave plasma reactor. The 10 mg/m^3 of the initial concentration of reactant was decomposed, and the removal efficiency obtained was as high as 98%. Steam was added to the process stream and eventually led to fewer by-products, which is a drawback of plasma rectors. A significant amount of tar contains soot, benzene derivative, and acetylene. With an increase in concentration from 167 to 1000 mg/m^3, the conversion efficiency decreases from 98% to 90% [82].

Table 2. Energy yield and beta value of various plasmas for different species in different plasma plate plasma reactors [107,108].

Molecules	Temperature (°C)	β (J/L)	Energy Cost eV/Molecule	Reactor Type
Methanol (100 ppm)	25.00	195.00	283.00	Pulsed Corona Reactor
Benzene (150 ppm)	25.00	671.00	1038.00	Pulsed Corona Reactor
Benzene (150 ppm)	300.00	138.00	214.00	Pulsed Corona Reactor
Dichloromethane (160 ppm)	25.00	1488.00	2159.00	Pulsed Corona Reactor
Dichloromethane (160 ppm)	300.00	46.00	67.00	Pulsed Corona Reactor
Methanol (400 ppm)	300.00	75.00	44.00	Pulsed Corona Reactor
Acetone (800 ppm)	25.00	3543.00	1028.00	Pulsed Corona Reactor
Acetone (800 ppm)	300.00	285.00	83.00	Pulsed Corona Reactor
ChloroBenzene (244 ppm)	180.00	102.00	97.00	Silent discharge Plasma Reactor
Styrene (407 ppm)	300.00	53.60	30.60	Silent discharge Plasma Reactor
Trichloroethylene (500 ppm)	25.00	12.40	5.80	Silent discharge Plasma Reactor
Styrene (814 ppm)	300.00	115.00	32.80	Silent discharge Plasma Reactor
Styrene (1627 ppm)	300.00	299.00	42.70	Silent discharge Plasma Reactor
Styrene (2441 ppm)	300.00	461.00	43.80	Silent discharge Plasma Reactor
Benzene (80 ppm)	25.00	277.00	83.00	Pulsed Corona Reactor
Toluene (100 ppm)	180.00	500.00	32.80	Pulsed Corona Reactor
Styrene (200 ppm)	300.00	1660.00	2159.00	Silent discharge Plasma Reactor

Researchers have recently focused their work on qualitative rather than quantitative measures. The authors of [95] highlighted the linear regression based on the available data to highlight the significance of modeling in terms of non-thermal plasma from almost 70 articles. A comprehensible relation has been found with up to 75% accuracy. The elucidated model maintains the performance based on the given conditions for particular compounds, particulate flow rates and removal efficiency based on specific input energy can be tabulated. A generalized formulation for a predictive model has been given for particular compound removal. The model translates the shortlisted generic performance for treating the VOC based on SEI, concentration inlet, temperature, and flow rate for the quantitative model.

$$Y = \beta_o + \beta_1 x_1 + \varepsilon \qquad (9)$$

Y is the dependent variable, β is the co-efficient, and x is the independent variable, either quantitatively or qualitatively. ε is the residual term. Based on the predictive model, a data analysis graph shows a synergy between EY_{actual} and $EY_{predicted}$. The predictive models presented in the literature provide a valuable tool for designing and optimizing plasma reactors to achieve high conversion rates and cleaner gas products. However, further research and development are required to explore more complex reactions and improve the performance of plasma-based tar removal systems for practical applications.

$$Energy\ Yield\ (EY)\tfrac{\text{g}}{\text{KWh}}$$
$$= \frac{[(Inlet\ Concnetration\ (C_{in}) - Outlet\ Concnetration\ (C_{out})\ ]}{(Specific\ Input\ Energy\ (SIE))} \tag{10}$$
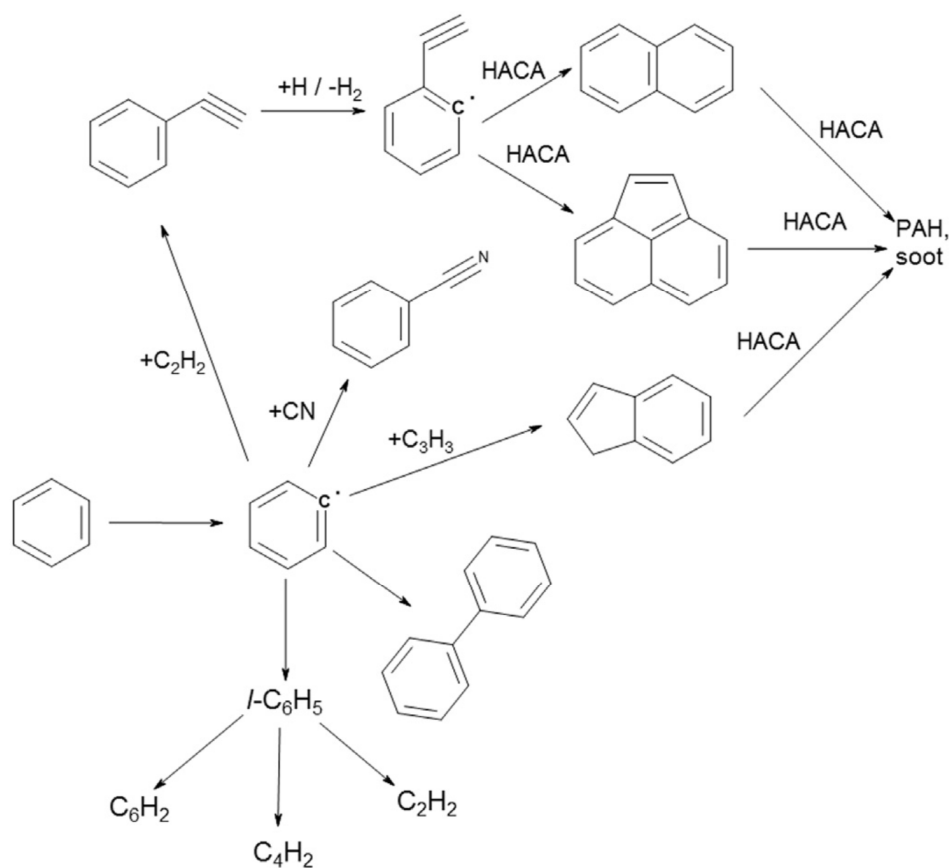

Figure 11. Benzene reaction generalized decomposition pathway—reprinted from [82] with permission from Elsevier.

7. Development and Validation of Kinetic Models for Hydrocarbon Conversion in Non-Thermal Plasma Reactors

In NTP reactions, the chemistry is of a very complex nature. Various plasma reactor types, including pulsed corona and silent discharge plasma reactors, have been investigated for the removal of volatile organic compounds (VOCs) such as benzene, toluene, and styrene. The kinetic models developed for these reactions have been validated against experimental data, and they provide valuable tools for predicting conversion rates and product yields under specific conditions. Usually, the focus is on the conversion of hydrocarbons, typically sighted by Nair as the "plasma CH_4 conversion race". The model combines experimental results into a sensitivity analysis required for the formation of oxygen at a temperature lower than 200 °C. Selectivity increases the total conversion, which in the model shows greater energy efficiency and lesser energy density. Hydrogen dissociation is complemented by water molecules in the reforming reaction within DBD reactors by

radical dissociation. The simple kinetic model involves perfect discharge assumption with no axial and radial direction reactions. A numerical model calculation incorporated the rate constant having a mixed phase and reaction phase. A pseudo-homogenous model is helpful for discharge chemistry. Thermal decomposition happens at the initial temperature point of T = 130–200 °C mainly due to gas composition. The model gives an energy density of 200 kJ/mol. Reaction model conversion and experimental conversion are closely related, and a model is 95% validated [86]. The kinetic model consists of parameters defining the decomposition of toluene and available soot reduction. The model is the best fit for the irradiation behavior that increases the decomposition rate, and an average error is almost 5%. The kinetic model rate constant is calculated by integral methods based on the experimental data along with Arrhenius equations. The model has been extrapolated for the prediction of toluene conversion and total product yield. Activation energy lowers by 12 times while the resultant heating requirement for conversion as compared to the thermal reactor is six times less. The kinetic model is favorable for the non-reforming process conversion [109]. Figure 12 illustrates the reaction rate constants for step-by-step plasma kinetic modeling, providing a visual representation of the comprehensive analysis conducted in the study.
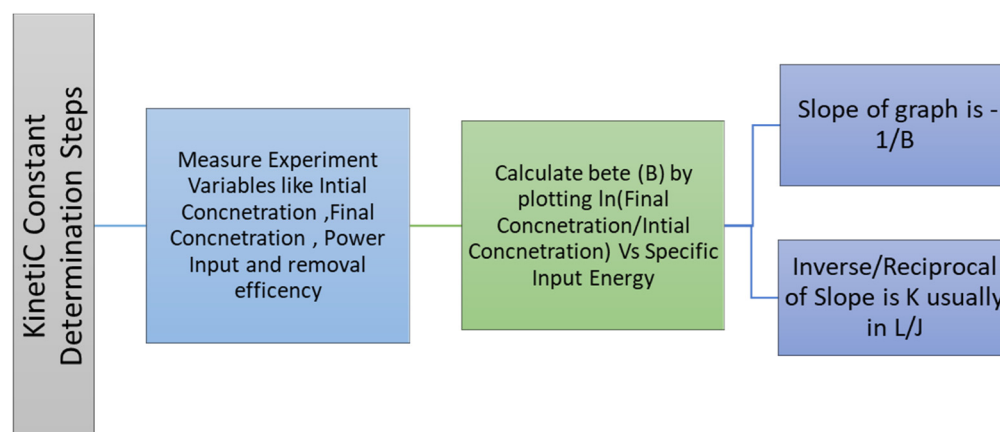

Figure 12. Reaction rate constant for step by step plasma kinetic modeling—based on [110].

NTP reactor schematics can be found in the work of Mei and Tu [111]. Abatement of benzene in the DBD reactor is carried out for conversion and by-product formation. Heterogenous phase products are analyzed using GC-MS at optimal specific energy densities. Benzonitriles, phenols, and amides are the main products that depend on SEDs and wt.% of carbon increase or decrease as its functions. At higher SED, products and VOCs are converted to CO_2. Solid-state products are morphologically studied under different SEDs [112].

$$EY = 3.6 \times \frac{M}{24.4} \times \frac{c_{in} - c_{out}}{SED} \tag{11}$$

M is the benzene molecular weight g/mol, 3.6 is the standard conversion factor, and the standard volume is 24.4 (L/mol) under normal conditions. The author describes a plasma gas phase reaction for benzene removal in which two benzene molecules are collided by excited electrons to form an intermediate derivative phenyl radical. Intermediate, unstable radicals undergo a brisk ring rupture that leads to a variety of radicals. Mainly, secondary benzene accommodates the gaseous pollutant with available collided electrons for the production of H, CO, O_3, NO_2, etc. VOC reacts with species for the finalized formation of CO_2 and H_2O [112].

8. Role of Energy Density and Efficiency in Plasma Discharge Kinetics Modeling and for Decomposition Reactions

The kinetic models have shed light on the reaction rates, intermediate species formation, and the role of active species in the plasma discharge. Advanced numerical simulations and software tools have been employed to simulate and validate the experimental results, providing a deeper understanding of the reaction mechanisms and the factors affecting tar removal efficiency. Moreover, statistical modeling techniques have been used to optimize reactor parameters and energy requirements, leading to improved performance and reduced pollutant emissions.

The integration of experimental studies, theoretical kinetic models, and numerical simulations has facilitated the development of efficient and environmentally friendly plasma-based tar removal technologies. These advancements have significant implications for various applications, including gasification processes, combustion systems, and waste treatment. The role of energy density and efficiency in plasma discharge kinetics modeling for decomposition reactions is highly important. Higher specific energy densities (SEDs) lead to increased decomposition efficiency, and various reaction pathways have been proposed to explain the breakdown of VOCs in different plasma reactors. The use of non-thermal plasma reactors has shown significant enhancement in the different gas mixture quality and increased VOC degradation. Plasma discharge accelerates the excited electrons for a unique range of 1 to 10 eV. In the literature, the C=C and C-C bond energies are 5.4 eV and correspond to 4.6 eV for the latter. Hence, an energy limit of 5.6 eV is required for the benzene ring dissociation, leading to breakdown, but somehow direct collision leads to different reactions, sometimes intermediate. SEDs increase from a value of 1.54 to 3.79 kJ/L for the required maximum decomposition efficiency of 59.98% to 96%. Unconverted liquid components such as benzene, ethylene, and benzonitrile are detected. Converted benzene results in CO_2. The solid phase contains phenols and esters, and their granularity is strongly dependent on SED increase, and a reduction in C wt.% is observed. The DBD reactor increases the mineralization phenomena for CO_2. A two-stage mechanism is observed involving direct electron collision with parent benzene molecule conversion and radical-induced conversion supported by NO3·, OH·, O·, and H· [112].

At a high temperature, producer gas containing benzene was subjected to a microwave reactor. The work has shown that carbon dioxide and hydrogen are vital ingredients in the syngas mixture quality enhancement and benzene degradation [60]. O, OH, and H are required for significant changes in the reaction components at the conversion rate of 98% [60]. Nitrogen contribution in naphthalene decomposition is relatively less due to the high dissociation energy of 9.8 eV as compared to oxygen 5.1 eV. An energy density of 75.5 J/L is obtained. A kinetic model based on semi-empirical kinetics for reaction rate constant is based on the log–log scale of concentration change for the residence time along the reaction zone of a non-plasma reactor at P = 0.07 W and 0.138 W for [92,113].

A self-consistent numerical model was developed for gas cleaning from naphthalene within the corona discharge reactor [114]. The reactor was divided into pre- and post-plasma chemical discharge processes. In pure nitrogen, the naphthalene decomposition rate was several folds bigger than that of the carrier gas mixture [114]. Two approaches to kinetic modeling have been proposed for pulse corona reactors. The first approach shows an infinitely fast and definite reaction occurring between available ions and molecules, so the G-value is classified for the primary neutral-charged species available. The secondary approach is uniquely based on the ions and electrons interaction for possible plasma chemical kinetics. In the case of naphthalene removal, N_2 is the prior one for removing enhancement, while H_2O decreases the removal rate and efficiency if added with N_2. Therefore, a charged species is utilized for cleaning process modification while the G-value is required for the primary non-charged active species [28].

Six benzene derivatives, along with an extra family formic acid, are being subjected to decomposition at ambient conditions in the plasma catalyst discharge system. GHSV range has been 11,000–55,000 h^{-1}. A global kinetic model shows that 6 VOCs are mainly

decomposed by SIE, while residence time, ionization potential, and GHSV have no effect on conversion. Five out of six show first-order kinetics. Only styrene behavior was found peculiar in nature. The K_e energy constant has been found from the kinetic model. Results show that the by-product formed is CO_2 and CO, and major CO_2 selectivity has been shown by formic acid (100%), whereas for others, it lies in the range of 70–75%. No catalyst deactivation has been found during decomposing hazardous compounds such as benzene and toluene [115]. In kinetic modeling, a log-plot illustrates the VOC conversion as a function of the independent variable for different power inputs [62]. At the same time, a semi-log plot demonstrates the reaction order and rate deduction for benzene in terms of SIE (Specific Energy Input) versus the concentration of carrier gases as given by Equation (12).

$$V_{inlet} - V_{out} = -K_e \times SIE \tag{12}$$

Pemen studied the global synthesis energy of plasma-prompted chemical reactions for VOC's pollution management. Assuming there are no critical extreme end reactions, direct collision reactions are important. Existing pollutant removal is only dependent on the plasma energy density, and the energy yield is constant. The current kinetic model removal rate demonstrates efficiency as the function of energy input density. Assuming that nonlinearity has a significant influence on plasma reactions. The removal rate is determined by the square base of the corona input energy density. These characteristics are investigated in the context of VOCs and generalized for other pollutants. Figure 13 shows a benzene decomposition semi-plot for power vs log concentration changes.
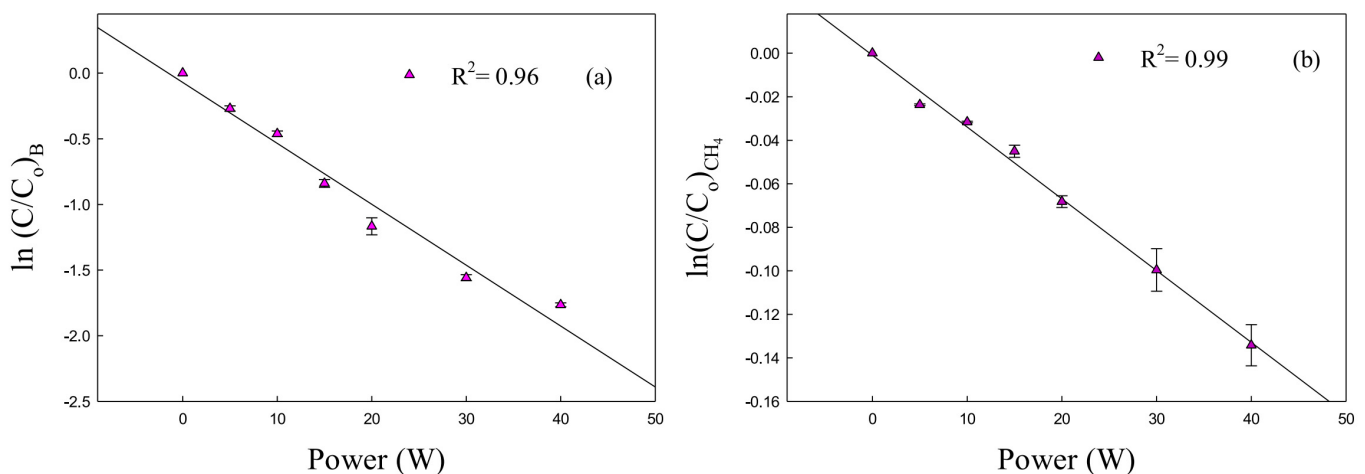

Figure 13. Benzene decomposition semi-plot for power vs log concentration changes—reprinted from [51] with permission from Elsevier; (**a**) ln (C/Co) vs. Power (benzene) (**b**) ln (C/C$_o$) vs. Power (CH$_4$).

An important question is how to combine a corona existing plasma reactor with a voltage-induced pulse generator to boost absolute energy productivity. An input voltage is identified for a given reactor to match a pulse generator. The voltage rising time, the result impedance of a pulse generator, and the depleted and sway capacitance of a reactor have all been improved. For example, the research looks at a 5.0 kW nonthermal plasma framework for NOx removal from exhaust gases. A simplified kinetic model for experimental results can be either exponential, linear, or square base, highly dependent on the reactor input energy density [116]. G is the standard calculator for the corona discharge reactors. It is defined as the energy cost per molecule removed for the energy yield. β is the specific energy, which increases as the G-value decreases with the removal efficiency. Whilst energy density decreases as energy cost decreases for the removal of molecules, total energy

yield increases accordingly. Increasing the corona energy density, the energy cost for each molecule *X* removal increases while the energy yield decreases [85,116,117].

$$\frac{X}{X_0} = \exp\left(-\frac{E}{\beta}\right) \tag{13}$$

Figure 14 presents the reactor modeling based on reactor performance in a silent discharge plasma reactor, illustrating the energy cost and beta value at different temperature zones for multiple concentrations of various pollutants.
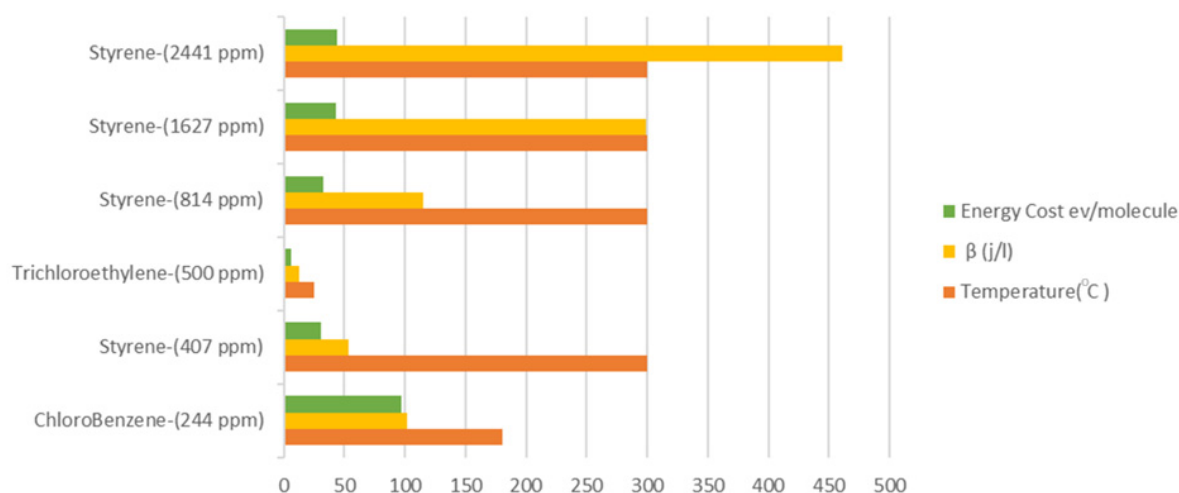

Figure 14. Reactor modeling based on reactor performant in silent discharger plasma reactor for energy cost, beta value at different temperature zones for multiple concentration of various pollutants—based on [108].

9. Kinetic Modeling and Energy Efficiency in a Non-Thermal Plasma Reactor for VOC Pollutant Removal and Management

In environmental chemistry, aerosol is a major pollutant for health concerns comprising a benzene ring compound. In AC/DC stream, benzene, toluene, and naphthalene are designated for decomposition in the corona discharge reactor. The linear kinetic model removal rate is shown by toluene and benzene in the corona discharge streamer, while styrene is a slow reactive species and shows an even trend for input power. Energy density lies in 27–32 J/L with a concentration factor of 9×10^5 cm^{-3} for benzene and toluene and is highest for styrene. Corona discharge is cost effective and leads to fewer by-products [107]. Comparative modeling for three gas streams, i.e., engine, methane combustion, and pollutant air, has been studied in two different reactors, i.e., the corona discharge reactor and silent barrier discharge reactor. Comparative modeling predicts the conversion and estimates the discharges [118]. Toluene is removed in a bi-gaseous mixture within a DBD reactor at less than 300 °C. The total wt.% of O_2 is kept at less than 10% and, at minimum, produces the overall best removal efficiency. H and O radicals increase removal rate because hydroxyl radical ions formed by recombination increase the removal rate. Three hydrocarbons, namely acetone, benzene, and ethane, when heated up to 300 °C to increase DBD reactor removal efficiency. Solid deposition has been confirmed by the plasma gas phase reaction. A simplified kinetic model of global nature is suggested by the author. Four-step reactions for available species, ions or radical R, are responsible for the pollutant removal. N_2 is regarded as the breakdown of species R for the reactions at different metastable states [102,110]. In Figure 15, a global generalized kinetic model for pollutant removal in a non-thermal plasma (NTP) reactor is presented, showcasing the comprehensive understanding and predictive capabilities achieved in the field of plasma-based tar removal and pollutant abatement.
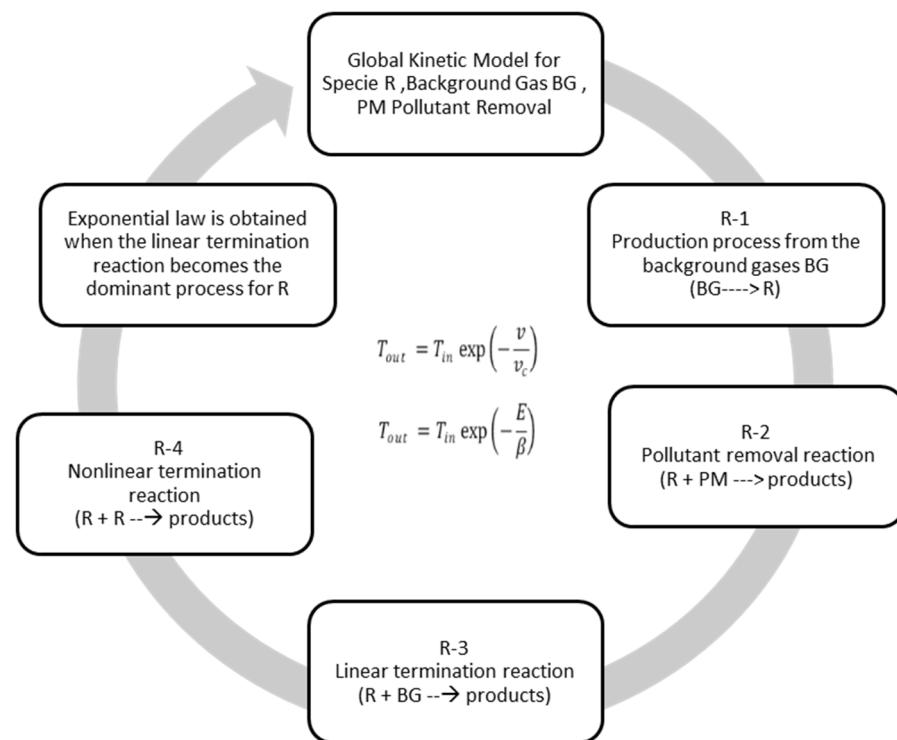
Figure 15. Global generalized kinetic model for pollutant removal in NTP reactor—based on [109].

T is the inlet and outlet concentration in ppm, v_c is the required characteristic frequency. Ozone formation is comparatively less as the oxygen density is kept constant in the range of 10^{14}–10^{15} cm^3 [119]. The tar decomposition kinetic model in the N$_2$ stream is interpreted based on irradiance, soot reduction, and experimental observations, not just single factor extrapolation, so results are more authentic. The proposed model is a baseline for future reactor design and optimization studies. Pre-exponential factors and temperature are kept constant for activation energy value deduction. Toluene chain reactions lead to radical formation in the decomposition initiation phase. Radicals react with more toluene molecules and lead to further radical propagation [109]. Figure 16 presents the suggested assumptions for the kinetic model, providing valuable insights into the complex reaction pathways involved in pollutant removal.
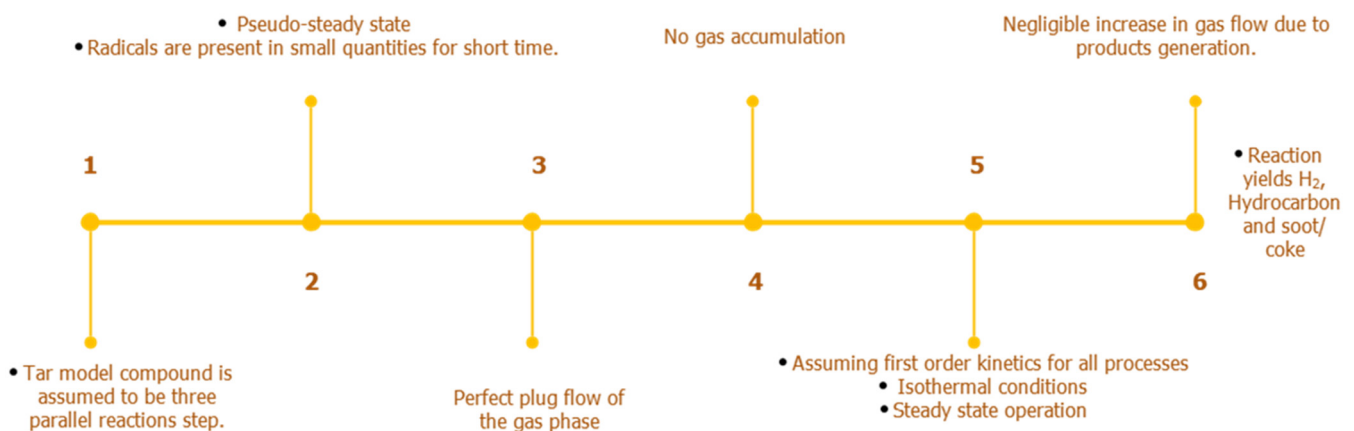

Figure 16. Suggested assumptions for kinetic model in tar removal in an NTP reactor—based on [109].

Predicted parameters verified the experimental data through the evaluation of model best fits, standard deviations, and sums of squares errors of a fitted parameter. The standard error of the estimate (SEE) or the combined residual variance is given in [95,109].

$F_{exp,i}$, $F_{mod,i}$, and n are the product yield and number of readings, respectively, by experimental and estimated.

$$SEE = \sqrt{\frac{\sum_i^n \left(F_{exp,i} - F_{mod,i}\right)^2}{n-2}} \tag{14}$$

Figure 17 illustrates the application of machine learning and numerical analysis in kinetic modeling to predict experimental outcomes. Kinetic modeling plays a crucial role in understanding and optimizing the behavior of complex reactions, such as tar decomposition in plasma reactors. However, accurately predicting the reaction rates and intermediate species formation can be challenging due to the intricate nature of the plasma discharge process. To address this challenge, researchers have integrated machine learning techniques with numerical analysis to enhance the predictive capabilities of kinetic models. Machine learning algorithms, such as neural networks and support vector machines, are trained on a vast dataset of experimental results to identify patterns and relationships between input parameters and reaction outcomes. The numerical analysis then employs these trained models to predict the behavior of the plasma reactor under different conditions. By incorporating machine learning into kinetic modeling, scientists can obtain more accurate and reliable predictions for tar decomposition and pollutant removal in plasma-based systems. This approach not only improves the understanding of reaction mechanisms but also aids in optimizing reactor configurations and energy inputs to achieve higher efficiency and cleaner gas products. Figure 18 serves as a visual representation of this innovative approach, showcasing how machine learning and numerical analysis work together to advance the field of sustainable green energy and plasma technology.
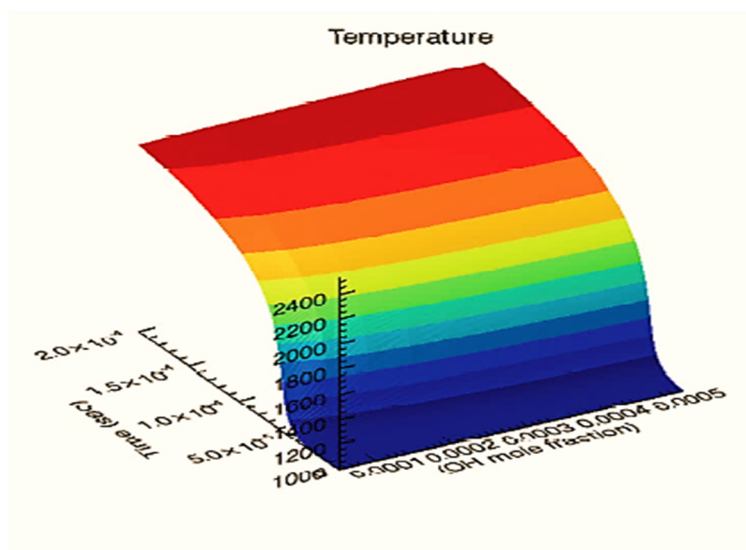

Figure 17. A General Numerical computation results for software calculations of kinetic model in terms of temperature and time along the reactor length.
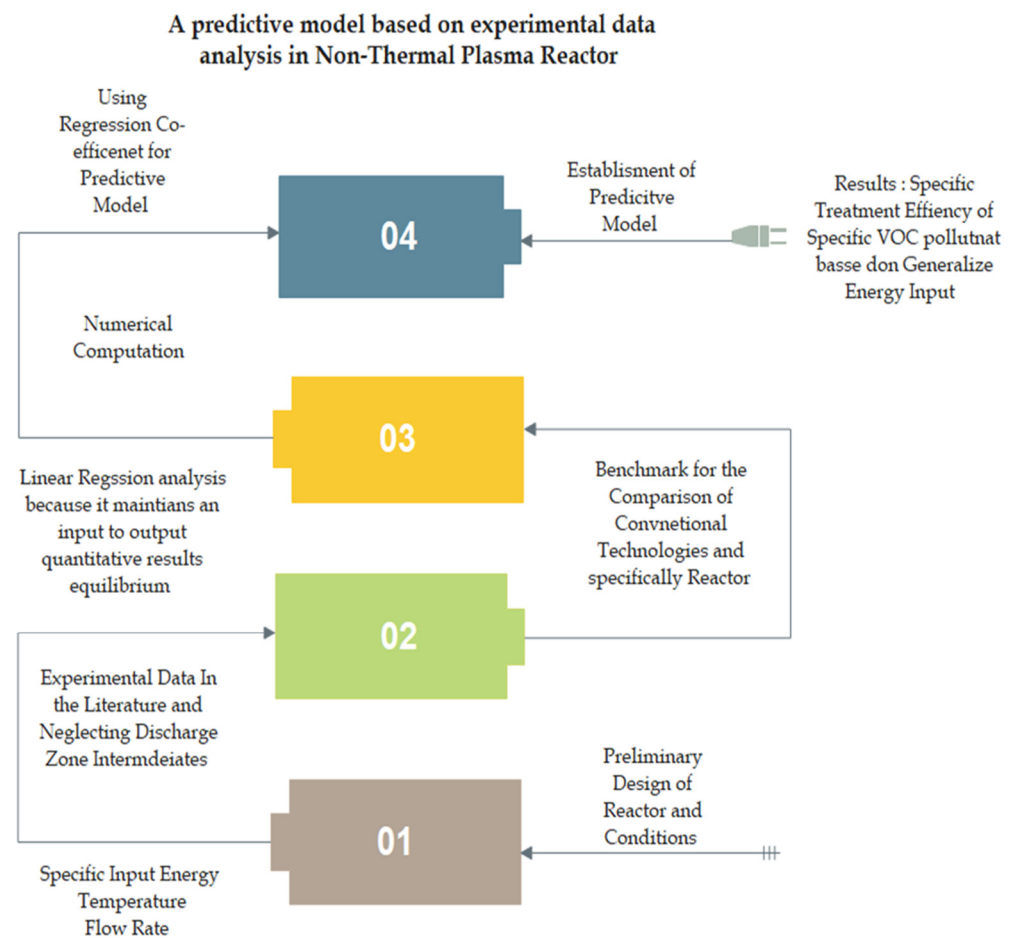
Figure 18. Predictive outcome for the experimental results for kinetic modeling using machine learning and numerical analysis—based on [95].

10. Kinetic Modeling for Tar Decomposition in a Plasma Reactor with Effects of Energy Density and Carrier Gases

An energy band of 7–8 eV is required for the gasifier product gas and pollutant removal in a cylindrical dielectric plasma reactor within $N_2 + O_2$ carrier gaseous mixture at a temperature of 350 K. In a DBD reactor, gas temperature increases substantially, thus not procuring many dangerous by-products. Reactor removal efficiency is 98%. The experimental and theoretical spectrum for an "Electron Energy Distribution Function (EEDF) model" comparison has been made, having ≤2% moisture content presence. Three stages of the chemical reduction procedure are presented [120].

- Defining chemical reactor discharge and Model Boltzmann kinetics on the basis of the main removal of analogue compound representative chemistry;
- Characterization studies: rotational temperature calculation based on optical emission spectroscopy;
- Average electron energy calculation for the second positive and first negative system discharge calculation for nitrogen molecules has been performed.

Based on the above three chemical reduction calculations, the mechanism has been assessed for generalized studies [70,120].

Chemkin (ANSYS 2022 R1) is good software for understanding the combustion behavior in plasma conditions for hydrocarbon and air mixtures. However, as the reaction kinetics becomes tedious, a greater amount of ion, radical-based kinetics data is required for the conversion calculation. At this point, this very viable software falls short. Chemkin is readily available due to the missing calculations of electric or magnetic fields in the plasma calculations [121]. Figure 18 illustrates general numerical computation results for software

calculations of the kinetic model, showcasing the temperature and time variations along the length of the reactor.

The second streamer limits the decomposition rate, and the temperature of the reaction process enhances the total conversion of analogue compounds. Energy consumption is effectively controlled by controlling the rate of radical propagation to minimise by-products that are usually unwanted carcinogenic. Thus, the gas distribution is increased with respect to the total flow rate of carrier gases [122]. A scheme of 57 species accounting for 308 reactions has been considered for tar removal in CO_2 carrier gas and validating reactions towards certain products. For mechanistic modeling, optical emission spectroscopy is utilized within experimentation that sheds light on reaction routes, products formed, and reaction rates based on emission spectra. Numerical kinetic modeling for the discharge process is conducted in two steps using the KINETICS program. Firstly, the kinetic equation is formed in the differential equation standard models. METAN 1.14 solves and integrates the differential equation model numerically. Data is extracted from NIST. To keep the computation easy, the system removes the C_4 greater hydrocarbon if not necessary [123]. Figure 19 illustrates the experimentation of plasma reactor and kinetic modeling, showcasing the formulation and simulation processes using open-source data, software tools, and numerical computation.
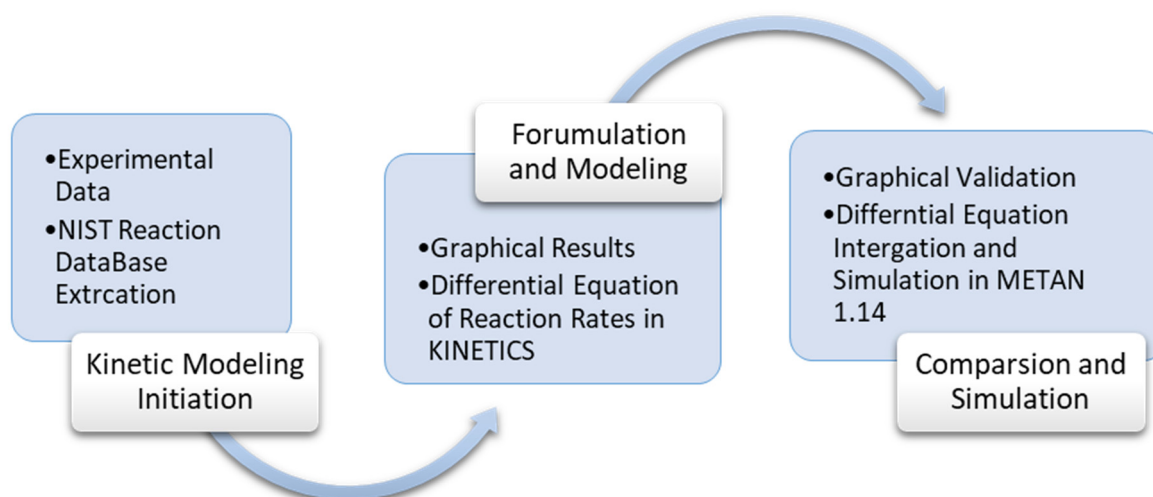

Figure 19. Experimentation of plasma reactor and kinetic modeling for formulation and simulation using open-source data.

11. Efficiency of Tar Removal in Pulse Discharge Reactors using NIST-Based Kinetic Modeling, and Numerical Simulation

Pemen proposed a synergistic resemblance of plasma with catalyst system as it usually reduces the severity of the process operational condition. NIST-based reaction data is used for deducing a model which curtails a large governance system for reaction conditioning. The streamer corona reactor has multiple frequencies of repetition for naphthalene as a tar model compound for removal efficiency studies. The simulation is bi-stage for gas cleaning. The initial stage is triggered by streamer propagation in a repetition sequence. Naphthalene is removed in carrier gaseous mixture of N_2, CO, H_2, and CO_2 of 50%, 20%, 12%, 17%, and 1% volumetrically [124]. The rate of streamer propagation is governed by the kinetic and transport of electrons and in photoionization leading to absorption of emitted radiation in the streamer head. The tar degradation that happens in nitrogen is similar to that in air, but photoionization in N_2 is double fold in comparison to air. The simulation proposed the G-value for the production of active species in the given mixture composition wights about

partial G-values. A tubular reactor is considered, which accounts for the dead zones, and the energy deposition is given in [115,124].

$$Wsyst = \frac{Ep}{Q} \times f \qquad (15)$$

340 elementary reaction contains almost 52 species in the tubular reactor, containing variables such as energy per pulse *Ep Q* flow rate and volume of the reactor. A specific energy influx per stream is

$$Wst = ne/Ge \qquad (16)$$

and the per cycle treatment is

$$N_{cv} = E_{sys}/W_{syst} \qquad (17)$$

while the temperature is kept constant.

Simulation of reaction species is performed in RADICAL software 3.7. The narrow type of streamer flow channel is non-uniform in nature and distributed along space, and energy is mainly discrete during several pulses. Models consider streamer spreading mainly due to disunion and the changing composition of gas in the background. Experimental and simulation comparison show a reaction is controlled mainly due to excited nitrogen molecules. Greater addition of nitrogen composition reduces the rate of removal [115,116,124]. The work [114] studied the conversion of naphthalene along with numerical simulations to build a self-consistent model having the impact of corona discharges with repeated pulses. H_2, CO, CO_2, and N_2 molecules present in the form of (N2(A3Σ)) dissociate to an excited state and decompose naphthalene for cleaning. Numerical simulation is divided into two concurrent stages based on experimentation conditions. Firstly, active species, i.e., ions, excited species, and radicals, are primarily generated within the discharge zone. In the secondary stage, a thin discharge filament plasma is generated by streamer and repeated propagations. Primary species have comparative densities and are required for the second-stage inputs for modeling studies showing chemical transformation usually induced by first-stage active species. RADICAL software incorporates tar conversion in a pulse reactor for kinetic modeling, which is a model for thin streamer input energy in the non-uniform spatial vicinity for active species inside the streamer reactor. Streamer models consider the traces and chemical compositions for modeling the sets of equations for different components n_j. Nitrogen with CO, CO_2, and H_2 decreases the removal rate and plays a pivotal role in gas cleaning. Electrons impact the dissociation for the further formation of nitrogenous compounds. Excited nitrogen molecules also add on to other tar compounds in addition to naphthalene at 770 K, with temperature having a substantial effect on removal efficiency. Removal efficiency, denoted by G increase, by T that shows T varies the rate constant.

Ber and Pemen studied the cracking of heavy hydrocarbon in a pulse discharge reactor, with heavy hydrocarbon generated from biogas. Portfolio has the capability of operating at high temperatures with a voltage of 100 kV and repeated pulse rate of 600–150 per second. At 1.5 kW of average power, cracked hydrocarbon tar is of a gaseous nature at 1 bar pressure and within a high temperature for a 0.25 m diameter and 3 m long stainless-steel corona wire along the axis. Product gas thermodynamics and kinetics are strongly dependent on contained C, O, H, and N contents, as well as pressure, and temperature. Tar compounds produced concentration and composition on the equilibrium conditions, i.e., pyrene concentration equilibrium decreases as biogas temperature increases. The author proposes a first-order kinetic model for heavy hydrocarbon removal at 200 °C. In N_2 presence, tar is cracked by a combined corona pulsed reactor with a range of 39 J/L to 154 J/L energy densities. Power input converts higher hydrocarbon to syngas [75,125]. The results of heavy and light tar removal by pulsed corona in the outlet of a real wood-fueled gasifier (BTG Almelo, Enschede, The Netherlands) are illustrated in Figure 20.

The Langmuir–Hinshelwood relation plays a crucial role in understanding the nitric reaction kinetics within a minimized photocatalytic continuous microreactor. This kinetic

model enables the validation of mass transfer processes, particularly the oxidation steps essential for the efficient removal of air pollutants and tar. Unlike previous models that primarily focused on end products, this model emphasizes the symmetry and comprehensive study of the byproducts formed during the reaction. By considering the complete reaction pathway, including the intermediate species and byproducts, a more accurate representation of the oxidation process and its associated kinetics is achieved. This enhanced understanding allows for better optimization of the photocatalytic microreactor design and operation, ultimately leading to improved energy efficiency and pollutant removal efficiency [91]. Figure 21 shows the mass transfer nexus with kinetic modeling in the non-thermal plasma reactor mechanism.
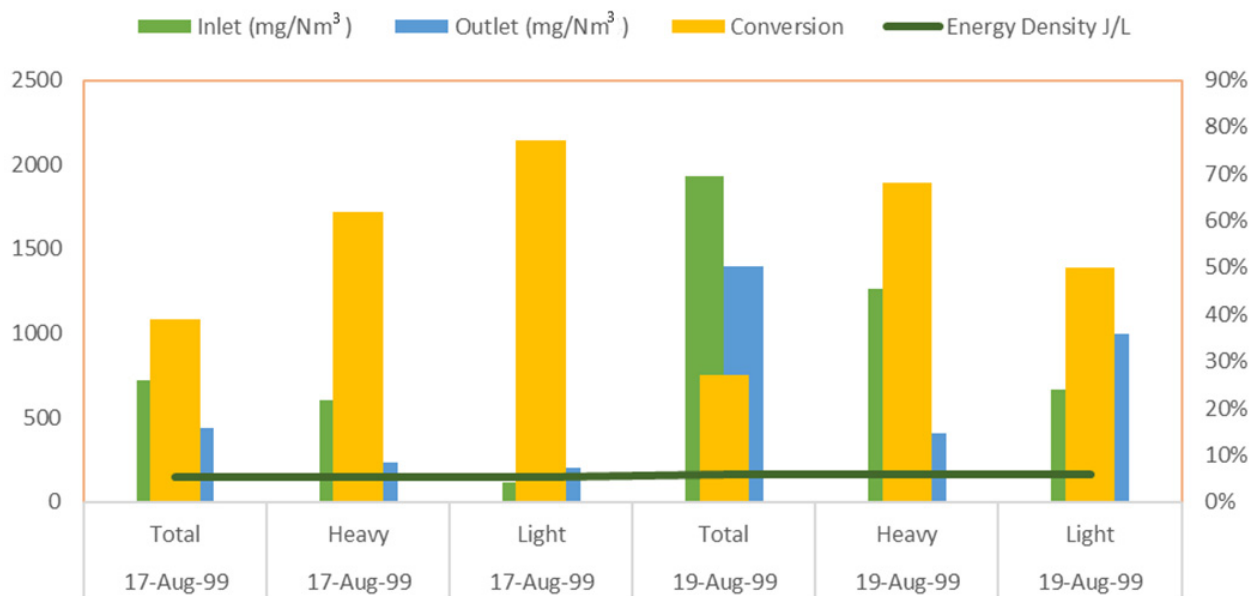

Figure 20. Results of heavy and light tar removal by pulsed corona in the outlet of a real wood-fueled gasifier (BTG Almelo, The Netherlands)—based on [125].
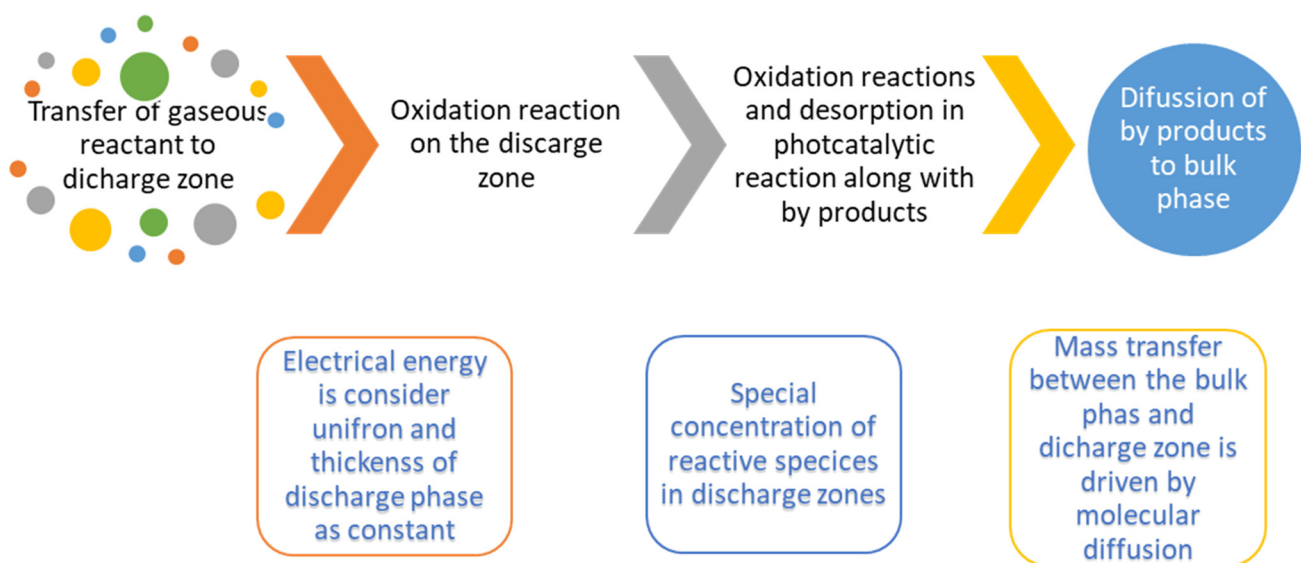

Figure 21. Mass transfer nexus with kinetic modeling in non-thermal plasma reactor mechanism—based on [91].

12. Effect of Temperature and Gas Composition on Tar Removal Efficiency in NTP and Pulsed Corona Discharge Reactors using Kinetic Modeling and Statistical Analysis

The studies presented in the literature demonstrate the potential of kinetic modeling and numerical simulation techniques in enhancing the performance of plasma reactors for tar removal and pollutant abatement, contributing to a greener and more sustainable approach to gas cleaning and energy conversion. As technology continues to evolve, more comprehensive and accurate models are expected to be developed, leading to even more efficient and effective plasma-based tar decomposition systems in the future. Higher temperature opens the toluene ring as it provides a thermal path in H_2 as it is a major product in steam gasifiers. A maximum temperature of 400 °C increases selectivity towards lower hydrocarbon at a residence time of 4.23 s. Methane, ethane, and benzene are produced in the majority, replacing the solid residue soot for an increase in temperature, but do not readily increase the conversion of toluene. NTP DBD reactor removal efficiency can be increased to 99% [65]. Benzene derivatives, along with formic acid, have been subjected to destruction in the plasma reactor having a catalyst bed. A simplified zero-order kinetic model has been proposed based on a specific input energy stream except for styrene. Gas hourly velocity and SIE are variable parameters during experimentation ranging from 11,000 to 55,000 h^{-1}. Intermediate is usually a formic acid compound leading all aromatic towards greater CO_2 formation. In a plasma reactor, no concrete relationship has been developed for the ionization and decomposition potential. In NTP reactors, reactions are driven by energy input and are mainly dependent on the gas residence time in the reactor/discharge region. Therefore, they have a short residence time [126]. Figure 22 represents the calculated reaction constant Ke for different VOCs based on kinetic modeling in NTP reactors.
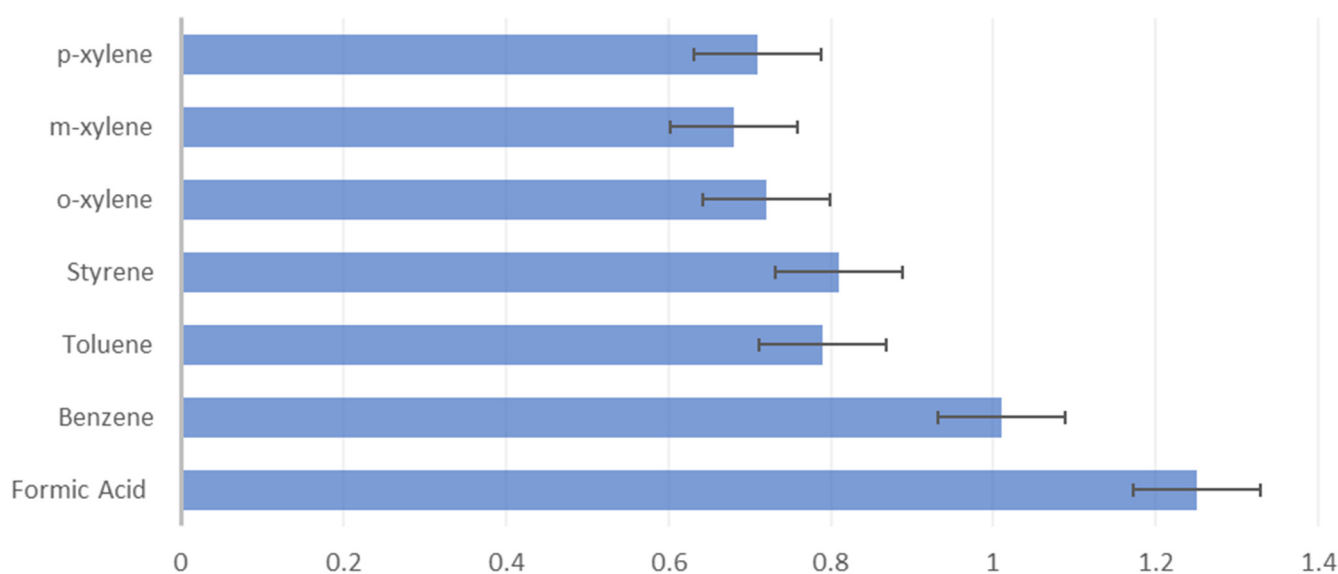

Figure 22. Reaction experimental constant for different VOCs based on the NTP reactor kinetic decomposition—based on [126].

Plug flow module for a tar reforming of heavy hydrocarbons for tube reactor at a temperature of almost 1400 °C for simulating bench-scale experimentation replica in CHEMKIN software using a set of reactions. Three test cases are compared with the modeling results. Two hundred fifty-seven reactions from the NIST website were fitted for a built-in kinetic model. The geometry of the tube reactor is shown in Figure 23. Two case studies were defined based on the light and heavy hydrocarbons in the case of toluene; benzene was considered lighter tar, and naphthalene was a heavier hydrocarbon. In comparison, pyrene was considered an alternative lighter tar in the second case, while naphthalene remained the heavy tar representative [93].

The physical methods are usually producing the liquid wastewater stream due to condensation at filters and bio-scrubbers. The high temperature of the thermal plasma reactor processes the gas with lower enthalpy. Corona discharges use 20% of the total input power for reducing a 50% inlet concentration at a temperature of 200 °C. The experimentation and kinetic model showed a harmony of 80%, mainly showing a deviation at a higher rate of conversion. The meshing of definite sizes for the syngas inlet and oxygen plasma has been studied for various conditions [86,117]. Figure 23 shows computational fluid dynamics based on the derived reactor kinetic model of an NTP reactor for syngas and oxygen plasma.
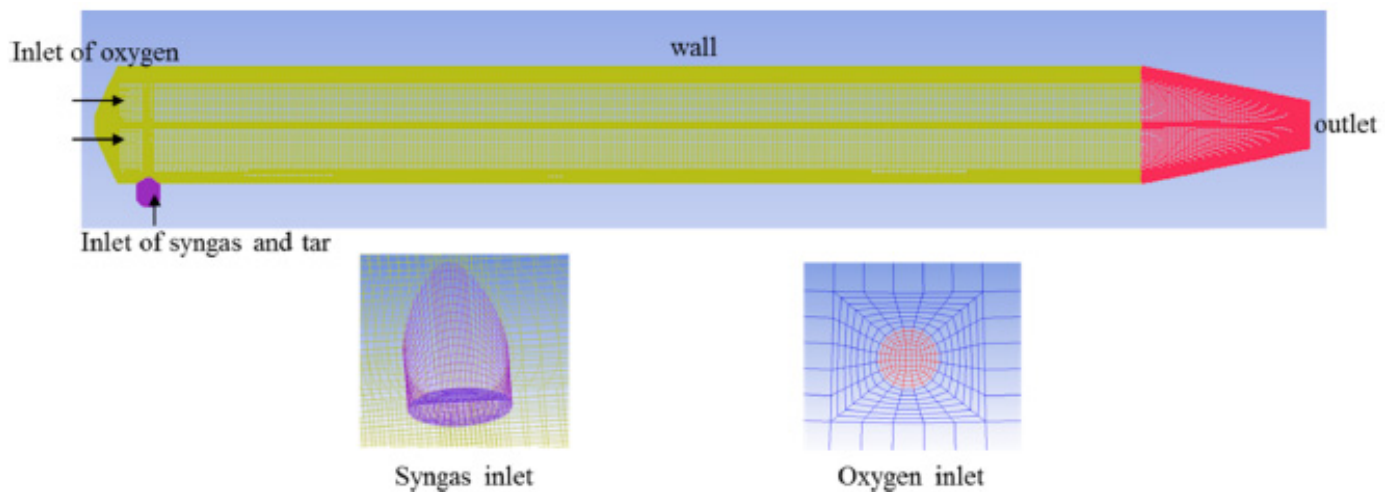

Figure 23. Computational fluid dynamics based on derived reactor kinetic model of an NTP reactor for syngas and oxygen plasma—reprinted from [104] with permission from Elsevier.

Statistical modeling tools such as parametric and factorial tests with response surface methodology are incorporated for the studies of gasifier product gas. These tests utilized the experiment conditions for giving the optimal requirements of reactors at a specified minimum specific energy (kJ/mol) [90,91,127–129]. A mixture of methane and carbon dioxide, 50% each, was simulated in a reactor with a minimum energy requirement of 184 kJ/mol. The gas gives forth a reformate composition, having a 24% hydrogen yield, selectivity of 47.8%, and an efficiency of 25.3% in comparison to a gliding arc plasma reactor. The main effects were input variables such as (equivalence ratio) EQR, steam to carbon ratio (SCR), and power inputs interaction in between. Assuming a first-order effect that increases in EQR significantly, a reverse effect on all other performance parameters and a positive effect on the conversion variable was observed.

The central composite method incorporates the central points and corner points from a factorial test for response surface methodology and optimization. The factorial test gave an optimal condition-determined energy requirement of 1.91 eV/H_2 molecule. The RSM approach is dependent on the feedstock conditions. The −1 to +1 shows the extreme and minimum points for defining the center points [68]. Optimization techniques in NTP reactors are shown in Figure 24.

The integration of experimental studies, theoretical kinetic models, and numerical simulations has facilitated the development of efficient and environmentally friendly plasma-based tar removal technologies. These advancements have significant implications for various applications, including gasification processes, combustion systems, and waste treatment. However, challenges still remain in the development of kinetic models for more complex reactions involving higher hydrocarbons and diverse gas compositions. Additionally, further research is required to address the limitations of existing software tools and numerical methods in accurately representing ion and radical-based kinetics.
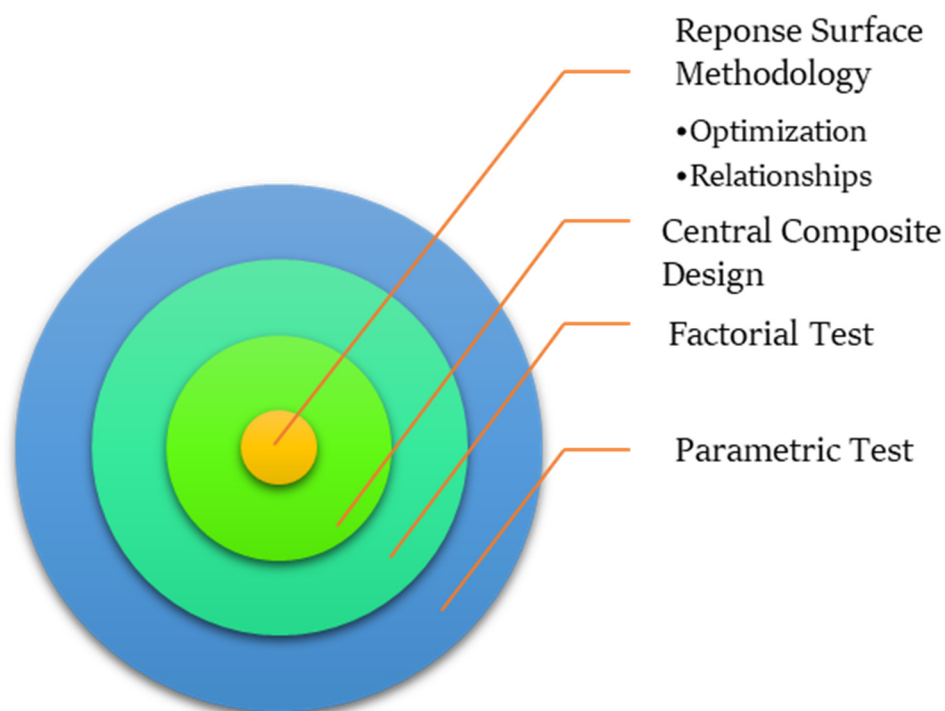
Figure 24. Optimization of reactor kinetics parameters using optimization techniques—based on [68].

In considering the future research direction of this field, it becomes apparent that plasma-based technologies are poised to play an increasingly pivotal role in the quest for sustainable and clean energy solutions. As we look ahead, it is imperative to channel our efforts into areas such as advanced plasma reactor design, precision control of plasma parameters, and the development of novel plasma catalysts. These endeavors will not only bolster the efficiency and effectiveness of plasma-based processes but also extend their applicability to diverse domains, including carbon capture and utilization, hydrogen production, and waste-to-energy conversion. Moreover, research should continue to focus on unraveling the intricacies of plasma–tar interactions, with a view to refining tar cracking and reforming processes. Understanding these mechanisms at a fundamental level will enable the design of more efficient and selective plasma reactors for tar removal. Additionally, the field would benefit from interdisciplinary collaborations that bridge the gap between plasma physics, materials science, and chemical engineering, fostering innovative approaches to address pressing global challenges. The future research landscape of plasma-based technologies holds tremendous promise. By harnessing the full potential of plasma, we can aspire to revolutionize the energy and environmental sectors, realizing a cleaner and more sustainable future. Collaboration, innovation, and a commitment to advancing our understanding of plasma processes will be central to achieving these objectives and shaping a greener energy landscape for generations to come. As technology continues to evolve, more comprehensive and accurate models are expected to be developed, leading to even more efficient and effective plasma-based tar decomposition systems in the future.

13. Conclusions

In conclusion, the role of experimental, modeling, and simulation studies of plasma in sustainable green energy is vital for advancing the field of renewable energy and promoting a cleaner, more sustainable future. Plasma-based technologies offer promising solutions for waste disposal and clean energy generation, making them essential components of a greener energy landscape. This comprehensive review discussed the diverse applications of plasma, with a particular focus on plasma combustion and gasification, as well as the efficient removal of tar in biomass-oriented technologies. The integration of experimental studies and theoretical modeling has provided valuable insights into plasma kinetics, reactor

optimization, and tar removal processes. Kinetic modeling and simulation techniques have played a crucial role in enhancing system efficiency, reducing emissions, and expanding the utilization of renewable energy sources. This study also highlighted the importance of understanding the mechanisms and reactivity of tar cracking and reforming for efficient tar conversion and removal. Furthermore, this review emphasized the significance of energy density and efficiency in plasma discharge kinetics modeling for decomposition reactions, which is essential for designing more effective plasma reactors. The research presented a roadmap for developing cleaner and more sustainable plasma-based solutions, contributing to the global efforts to address climate change and environmental crises. As we continue to explore and advance plasma-based technologies, a collaboration between experimentalists, modelers, and researchers from various disciplines is essential. This concerted effort will be instrumental in achieving the objectives set forth in global initiatives, such as the Paris Climate Accord and COP 24, and creating a greener energy landscape for generations to come.

Abbreviations

AC	alternating current
CCS	carbon capture and storage
CSTR	continuously stirred tank reactor
DBD	dielectric-barrier discharge
DC	direct current
ECN	Energy Centre of Netherlands (nowadays called TNO)
EQR	equivalence ratio
EEDF	electron energy distribution function
GC-MS	gas chromatography—mass spectroscopy
GHSV	Gas Hourly Space Velocity
LHV	lower heating value
MC	moisture content
NIST	national institute of standards and technology
NTP	non-thermal plasma
PAH	poly-aromatic hydrocarbons
PFR	plug flow reactor
RSM	response surface methodology
SCR	steam to carbon ratio
SED	specific energy density
SIE	specific input energy
VOC	volatile organic compounds

References

1. Tzelepi, V.; Zeneli, M.; Kourkoumpas, D.-S.; Karampinis, E.; Gypakis, A.; Nikolopoulos, N.; Grammelis, P. Biomass Availability in Europe as an Alternative Fuel for Full Conversion of Lignite Power Plants: A Critical Review. *Energies* **2020**, *13*, 3390. [CrossRef]

2. Qvist, S.; Gładysz, P.; Bartela, Ł.; Sowiżdżał, A. Retrofit Decarbonization of Coal Power Plants—A Case Study for Poland. *Energies* **2021**, *14*, 120. [CrossRef]

3. Balode, L.; Zlaugotne, B.; Gravelsins, A.; Svedovs, O.; Pakere, I.; Kirsanovs, V.; Blumberga, D. Carbon Neutrality in Municipalities: Balancing Individual and District Heating Renewable Energy Solutions. *Sustainability* **2023**, *15*, 8415. [CrossRef]

4. Liobikienė, G.; Miceikienė, A. Contribution of the European Bioeconomy Strategy to the Green Deal Policy: Challenges and Opportunities in Implementing These Policies. *Sustainability* **2023**, *15*, 7139. [CrossRef]

5. Piersa, P.; Szufa, S.; Czerwińska, J.; Ünyay, H.; Adrian, Ł.; Wielgosinski, G.; Obraniak, A.; Lewandowska, W.; Marczak-Grzesik, M.; Dzikuć, M.; et al. Pine Wood and Sewage Sludge Torrefaction Process for Production Renewable Solid Biofuels and Biochar as Carbon Carrier for Fertilizers. *Energies* **2021**, *14*, 8176. [CrossRef]

6. Romanowska-Duda, Z.; Szufa, S.; Grzesik, M.; Piotrowski, K.; Janas, R. The Promotive Effect of Cyanobacteria and Chlorella sp. Foliar Biofertilization on Growth and Metabolic Activities of Willow (*Salix viminalis* L.) Plants as Feedstock Production, Solid Biofuel and Biochar as C Carrier for Fertilizers via Torrefaction Process. *Energies* **2021**, *14*, 5262.

7. Szufa, S.; Piersa, P.; Junga, R.; Błaszczuk, A.; Modliński, N.; Sobek, S.; Marczak-Grzesik, M.; Adrian, Ł.; Dzikuć, M. Numerical modeling of the co-firing process of an in situ steam-torrefied biomass with coal in a 230 MW industrial-scale boiler. *Energy* **2023**, *263*, 125918. [CrossRef]

8. Piersa, P.; Unyay, H.; Szufa, S.; Lewandowska, W.; Modrzewski, R.; Ślężak, R.; Ledakowicz, S. An Extensive Review and Comparison of Modern Biomass Torrefaction Reactors vs. Biomass Pyrolysis—Part 1. *Energies* **2022**, *15*, 2227. [CrossRef]

9. Devi, L.; Ptasinski, K.J.; Janssen, F.J.J.G. A review of the primary measures for tar elimination in biomass gasification processes. *Biomass Bioenergy* **2003**, *24*, 125–140. [CrossRef]

10. Gładysz, P.; Strojny, M.; Bartela, Ł.; Hacaga, M.; Froehlich, T. Merging Climate Action with Energy Security through CCS—A Multi-Disciplinary Framework for Assessment. *Energies* **2023**, *16*, 35. [CrossRef]

11. Ziółkowski, P.; Głuch, S.; Ziółkowski, P.J.; Badur, J. Compact High Efficiency and Zero-Emission Gas-Fired Power Plant with Oxy-Combustion and Carbon Capture. *Energies* **2022**, *15*, 2590. [CrossRef]

12. Ziółkowski, P.; Madejski, P.; Amiri, M.; Kuś, T.; Stasiak, K.; Subramanian, N.; Pawlak-Kruczek, H.; Badur, J.; Niedźwiecki, Ł.; Mikielewicz, D. Thermodynamic Analysis of Negative CO2 Emission Power Plant Using Aspen Plus, Aspen Hysys, and Ebsilon Software. *Energies* **2021**, *14*, 6304. [CrossRef]

13. Stavrakas, V.; Spyridaki, N.-A.; Flamos, A. Striving towards the Deployment of Bio-Energy with Carbon Capture and Storage (BECCS): A Review of Research Priorities and Assessment Needs. *Sustainability* **2018**, *10*, 2206. [CrossRef]

14. Čespiva, J.; Niedzwiecki, L.; Vereš, J.; Skřínský, J.; Wnukowski, M.; Borovec, K.; Ochodek, T. Evaluation of the performance of the cross/updraft type gasification technology with the sliding bed over a circular grate. *Biomass Bioenergy* **2022**, *167*, 106639. [CrossRef]

15. Čespiva, J.; Skřínský, J.; Vereš, J.; Wnukowski, M.; Serenčíšová, J.; Ochodek, T. Solid recovered fuel gasification in sliding bed reactor. *Energy* **2023**, *278*, 127830. [CrossRef]

16. Koido, K.; Takata, E.; Yanagida, T.; Kuboyama, H. Techno-Economic Assessment of Heat Supply Systems in Woodchip Drying Bases for Wood Gasification Combined Heat and Power. *Sustainability* **2022**, *14*, 16878. [CrossRef]

17. Čespiva, J.; Skřínský, J.; Vereš, J.; Borovec, K.; Wnukowski, M. Solid-recovered fuel to liquid conversion using fixed bed gasification technology and a Fischer–Tropsch synthesis unit–Case study. *Int. J. Energy Prod. Manag.* **2020**, *5*, 212–222. [CrossRef]

18. Čespiva, J.; Niedzwiecki, L.; Wnukowski, M.; Krochmalny, K.; Mularski, J.; Ochodek, T.; Pawlak-Kruczek, H. Torrefaction and gasification of biomass for polygeneration: Production of biochar and producer gas at low load conditions. *Energy Rep.* **2022**, *8*, 134–144. [CrossRef]

19. Manga, M.; Aragón-Briceño, C.; Boutikos, P.; Semiyaga, S.; Olabinjo, O.; Muoghalu, C.C. Biochar and Its Potential Application for the Improvement of the Anaerobic Digestion Process: A Critical Review. *Energies* **2023**, *16*, 4051. [CrossRef]

20. Sieradzka, M.; Mlonka-Mędrala, A.; Kalemba-Rec, I.; Reinmöller, M.; Küster, F.; Kalawa, W.; Magdziarz, A. Evaluation of Physical and Chemical Properties of Residue from Gasification of Biomass Wastes. *Energies* **2022**, *15*, 3539. [CrossRef]

21. Výtisk, J.; Čespiva, J.; Jadlovec, M.; Kočí, V.; Honus, S.; Ochodek, T. Life cycle assessment applied on alternative production of carbon-based sorbents—A comparative study. *Sustain. Mater. Technol.* **2023**, *35*, e00563. [CrossRef]

22. Čespiva, J.; Jadlovec, M.; Výtisk, J.; Serenčíšová, J.; Tadeáš, O.; Honus, S. Softwood and solid recovered fuel gasification residual chars as sorbents for flue gas mercury capture. *Environ. Technol. Innov.* **2023**, *29*, 102970. [CrossRef]

23. Sieradzka, M.; Mlonka-Mędrala, A.; Magdziarz, A. Comprehensive investigation of the CO2 gasification process of biomass wastes using TG-MS and lab-scale experimental research. *Fuel* **2022**, *330*, 125566. [CrossRef]

24. Werle, S.; Dudziak, M. Analysis of Organic and Inorganic Contaminants in Dried Sewage Sludge and By-Products of Dried Sewage Sludge Gasification. *Energies* **2014**, *7*, 462–476. [CrossRef]

25. Ferreira, S.; Monteiro, E.; Brito, P.; Castro, C.; Calado, L.; Vilarinho, C. Experimental Analysis of Brewers' Spent Grains Steam Gasification in an Allothermal Batch Reactor. *Energies* **2019**, *12*, 912. [CrossRef]

26. Wnukowski, M.; Moroń, W. Warm Plasma Application in Tar Conversion and Syngas Valorization: The Fate of Hydrogen Sulfide. *Energies* **2021**, *14*, 7383. [CrossRef]

27. Bityurin, V.; Filimonova, E.; Naidis, G. Mechanisms of Conversion of Heavy Hydrocarbons in Biogas Initiated by Pulsed Corona Discharges. In *Plasma Assisted Decontamination of Biological and Chemical Agents*; Springer: Dordrecht, The Netherlands, 2008; pp. 135–142.

28. Filimonova, E.; Naidis, G. Effect of gas mixture composition on tar removal process in a pulsed corona discharge reactor. *J. Phys. Conf. Ser.* **2010**, *257*, 012018. [CrossRef]

29. Zigan, L. Overview of Electric Field Applications in Energy and Process Engineering. *Energies* **2018**, *11*, 1361. [CrossRef]

30. Leonov, S.B. Electrically Driven Supersonic Combustion. *Energies* **2018**, *11*, 1733. [CrossRef]

31. Tholin, F.; Lacoste, D.; Bourdon, A. Influence of fast-heating processes and O atom production by a nanosecond spark discharge on the ignition of a lean H2H2–air premixed flame. *Combust. Flame* **2014**, *161*, 1235–1246. [CrossRef]

32. Zare, S.; Lo, H.W.; Askari, O. Flame Stability in Inverse Coaxial Injector Using Repetitive Nanosecond Pulsed Plasma. *J. Energy Resour. Technol.* **2020**, *142*, 082101. [CrossRef]

33. Lacoste, D.; Moeck, J.; Roberts, W.; Chung, S.; Cha, M.S. Analysis of the step responses of laminar premixed flames to forcing by non-thermal plasma. *Proc. Combust. Inst.* **2016**, *36*, 4145–4153. [CrossRef]

34. Mączka, T.; Pawlak-Kruczek, H.; Niedzwiecki, L.; Ziaja, E.; Chorążyczewski, A. Plasma Assisted Combustion as a Cost-Effective Way for Balancing of Intermittent Sources: Techno-Economic Assessment for 200 MWel Power Unit. *Energies* **2020**, *13*, 5056. [CrossRef]

35. Messerle, V.; Karpenko, E.; Ustimenko, A.; Lavrichshev, O. Plasma preparation of coal to combustion in power boilers. *Fuel Process. Technol.* **2013**, *107*, 93–98. [CrossRef]

36. Bukowski, P.; Kobel, P.; Kordylewski, W.; Mączka, T. Use of cavity plasmatron in pulverized coal muffle burner for start-up of a boiler. *Rynek Energii* **2010**, *86*, 132–136.

37. Karpenko, E.; Messerle, V.; Ustimenko, A. Plasma-aided solid fuel combustion. *Proc. Combust. Inst.* **2007**, *31*, 3353–3360. [CrossRef]

38. Messerle, V.; Karpenko, E.; Ustimenko, A. Plasma assisted power coal combustion in the furnace of utility boiler: Numerical modeling and full-scale test. *Fuel* **2014**, *126*, 294–300. [CrossRef]

39. Nur, M.; Sumariyah, S.; Suseno, A. Removal of emission gas COx, NOx and SOx from automobile using non-thermal plasma. In *IOP Conference Series: Materials Science and Engineering*; IOP Publishing: Bristol, UK, 2019; p. 012085.

40. Saeed, M.A.; Niedzwiecki, L.; Arshad, M.Y.; Skrinsky, J.; Andrews, G.E.; Phylaktou, H.N. Combustion and Explosion Characteristics of Pulverised Wood, Valorized with Mild Pyrolysis in Pilot Scale Installation, Using the Modified ISO 1 m3 Dust Explosion Vessel. *Appl. Sci.* **2022**, *12*, 12928. [CrossRef]

41. Rafique, M.A.; Kiran, S.; Jamal, A.; Anjum, M.N.; Jalal, F.; Munir, B.; Hafiz, I.; Noureen, F.; Ajmal, S.; Ahmad, W.; et al. Green synthesis of copper nanoparticles using Allium cepa (onion) peels for removal of Disperse Yellow 3 dye. *Desalin. Water Treat.* **2022**, *272*, 259–265. [CrossRef]

42. Ramos, A.; Teixeira, C.A.; Rouboa, A. Environmental Assessment of Municipal Solid Waste by Two-Stage Plasma Gasification. *Energies* **2019**, *12*, 137. [CrossRef]

43. Mączka, T. *Technologia Plazmowego Zgazowania Biomasy i Odpadów Organicznych dla Wytwarzania Paliw Płynnych*; Wydawnictwo Książkowe Instytutu Elektrotechniki: Warsaw, Poland, 2014.

44. Messerle, V.E.; Mossé, A.L.; Ustimenko, A.B.; Slavinskaya, N.A.; Sitdikov, Z.Z. Recycling of Organic Waste in a Plasma Reactor. *J. Eng. Phys. Thermophys.* **2020**, *93*, 987–997. [CrossRef]

45. Messerle, V.E.; Mossé, A.L.; Paskalov, G.; Sitdikov, Z.Z.; Ustimenko, A.B. Plasma Chemical Conversion of Spent Lubricating Materials. *J. Eng. Phys. Thermophys.* **2021**, *94*, 1344–1356. [CrossRef]

46. Agon, N.; Hrabovský, M.; Chumak, O.; Hlína, M.; Kopecký, V.; Masláni, A.; Bosmans, A.; Helsen, L.; Skoblja, S.; Van Oost, G.; et al. Plasma gasification of refuse derived fuel in a single-stage system using different gasifying agents. *Waste Manag.* **2016**, *47*, 246–255. [CrossRef] [PubMed]

47. Vishwajeet; Pawlak-Kruczek, H.; Baranowski, M.; Czerep, M.; Chorążyczewski, A.; Krochmalny, K.; Ostrycharczyk, M.; Ziółkowski, P.; Madejski, P.; Mączka, T.; et al. Entrained Flow Plasma Gasification of Sewage Sludge–Proof-of-Concept and Fate of Inorganics. *Energies* **2022**, *15*, 1948. [CrossRef]

48. Ivanovska, A.; Milošević, M.; Obradović, B.; Svirčev, Z.; Kostić, M. Plasma Treatment as a Sustainable Method for Enhancing the Wettability of Jute Fabrics. *Sustainability* **2023**, *15*, 2125. [CrossRef]

49. Krochmalny, K.; Pawlak-Kruczek, H.; Skoczylas, N.; Kudasik, M.; Gajda, A.; Gnatowska, R.; Serafin-Tkaczuk, M.; Czapka, T.; Jaiswal, A.K.; Vishwajeet; et al. Use of Hydrothermal Carbonization and Cold Atmospheric Plasma for Surface Modification of Brewer's Spent Grain and Activated Carbon. *Energies* **2022**, *15*, 4396. [CrossRef]

50. Yar, A.; Arshad, M.Y.; Asghar, F.; Amjad, W.; Asghar, F.; Hussain, M.I.; Lee, G.H.; Mahmood, F. Machine Learning-Based Relative Performance Analysis of Monocrystalline and Polycrystalline Grid-Tied PV Systems. *Int. J. Photoenergy* **2022**, *2022*, 3186378. [CrossRef]

51. Saleem, F.; Abbas, A.; Rehman, A.; Khoja, A.H.; Naqvi, S.R.; Arshad, M.Y.; Zhang, K.; Harvey, A. Decomposition of benzene as a biomass gasification tar in CH4 carrier gas using non-thermal plasma: Parametric and kinetic study. *J. Energy Inst.* **2022**, *102*, 190–195. [CrossRef]

52. Yousaf, A.M.; Aqsa, R. Integrating Circular Economy, SBTI, Digital LCA, and ESG Benchmarks for Sustainable Textile Dyeing: A Critical Review of Industrial Textile Practices. *Glob. NEST J.* **2023**, *25*, 39–51. [CrossRef]

53. Gul, H.; Arshad, M.Y.; Tahir, M.W. Production of H2 via sorption enhanced auto-thermal reforming for small scale Applications-A process modeling and machine learning study. *Int. J. Hydrogen Energy* **2023**, *48*, 12622–12635. [CrossRef]

54. El-Tayeb, A.; El-Dein, A.Z.; Elnaggar, A.Y.; Hussein, E.E. Influence of Temperature in Degradation of Organic Pollution Using Corona Discharge Plasma. *Sustainability* **2021**, *13*, 12971. [CrossRef]

55. Rouwenhorst, K.H.; Engelmann, Y.; van't Veer, K.; Postma, R.S.; Bogaerts, A.; Lefferts, L. Plasma-driven catalysis: Green ammonia synthesis with intermittent electricity. *Green Chem.* **2020**, *22*, 6258–6287. [CrossRef]

56. Ioannou, I.; D'Angelo, S.C.; Galán-Martín, Á.; Pozo, C.; Pérez-Ramírez, J.; Guillén-Gosálbez, G. Process modelling and life cycle assessment coupled with experimental work to shape the future sustainable production of chemicals and fuels. *React. Chem. Eng.* **2021**, *6*, 1179–1194. [CrossRef]

57. Zhang, L.; Hu, X.; Wang, Z.; Sun, F.; Dorrell, D.G. A review of supercapacitor modeling, estimation, and applications: A control/management perspective. *Renew. Sustain. Energy Rev.* **2018**, *81*, 1868–1878. [CrossRef]

58. Oliveira, M.; Ramos, A.; Ismail, T.M.; Monteiro, E.; Rouboa, A. A Review on Plasma Gasification of Solid Residues: Recent Advances and Developments. *Energies* **2022**, *15*, 1475. [CrossRef]

59. Rafique, M.; Kiran, S.; Ashraf, A.; Mukhtar, N.; Rizwan, S.; Ashraf, M.; Arshad, M. Effective removal of direct orange 26 dye using copper nanoparticles synthesized from Tilapia fish scales. *Glob. NEST J.* **2022**, *24*, 311–317.

60. Wnukowski, M.; Jamróz, P. Microwave plasma treatment of simulated biomass syngas: Interactions between the permanent syngas compounds and their influence on the model tar compound conversion. *Fuel Process. Technol.* **2018**, *173*, 229–242. [CrossRef]

61. Zhenghui, L.; Zimei, H.; Yaya, S. New media environment, environmental regulation and corporate green technology innovation:Evidence from China. *Energy Econ.* **2023**, *119*, 106545. [CrossRef]

62. Tinghui, L.; Xue, L.; Gaoke, L. Business cycles and energy intensity. Evidence from emerging economies. *Borsa Istanb. Rev.* **2022**, *22*, 560–570. [CrossRef]

63. Valderrama Rios, M.L.; González, A.M.; Lora, E.E.S.; Almazán del Olmo, O.A. Reduction of tar generated during biomass gasification: A review. *Biomass Bioenergy* **2018**, *108*, 345–370. [CrossRef]

64. Rueda, Y.G.; Helsen, L. The role of plasma in syngas tar cracking. *Biomass Convers. Biorefinery* **2020**, *10*, 857–871. [CrossRef]

65. Saleem, F.; Zhang, K.; Harvey, A. Temperature dependence of non-thermal plasma assisted hydrocracking of toluene to lower hydrocarbons in a dielectric barrier discharge reactor. *Chem. Eng. J.* **2019**, *356*, 1062–1069. [CrossRef]

66. Čespiva, J.; Wnukowski, M.; Niedzwiecki, L.; Skřínský, J.; Vereš, J.; Ochodek, T.; Pawlak-Kruczek, H.; Borovec, K. Characterization of tars from a novel, pilot scale, biomass gasifier working under low equivalence ratio regime. *Renew. Energy* **2020**, *159*, 775–785. [CrossRef]

67. Nair, S.; Pemen, A.J.M.; Yan, K.; Heesch, E.J.M.; Ptasinski, K.; Drinkenburg, A.A.H. Chemical Processes in Tar Removal from Biomass Derived Fuel Gas by Pulsed Corona Discharges. *Plasma Chem. Plasma Process.* **2003**, *23*, 665–680. [CrossRef]

68. Mousavi, S.M.A.; Piavis, W.; Turn, S. Reforming of biogas using a non-thermal, gliding-arc, plasma in reverse vortex flow and fate of hydrogen sulfide contaminants. *Fuel Process. Technol.* **2019**, *193*, 378–391. [CrossRef]

69. Schmidt, M.; Jõgi, I.; Holub, M.; Brandenburg, R. Non-thermal plasma based decomposition of volatile organic compounds in industrial exhaust gases. *Int. J. Environ. Sci. Technol.* **2015**, *12*, 3745–3754. [CrossRef]

70. Li, Q.; Wang, Q.; Kayamori, A.; Zhang, J. Experimental study and modeling of heavy tar steam reforming. *Fuel Process. Technol.* **2018**, *178*, 180–188. [CrossRef]

71. Saleem, F.; Zhang, K.; Harvey, A. Role of CO_2 in the Conversion of Toluene as a Tar Surrogate in a Nonthermal Plasma Dielectric Barrier Discharge Reactor. *Energy Fuels* **2018**, *32*, 5164–5170. [CrossRef]

72. Saleem, F.; Harris, J.; Zhang, K.; Harvey, A. Non-thermal plasma as a promising route for the removal of tar from the product gas of biomass gasification—A critical review. *Chem. Eng. J.* **2020**, *382*, 122761. [CrossRef]

73. Affonso Nobrega, P.; Gaunand, A.; Rohani, V.; Cauneau, F.; Fulcheri, L. Applying chemical engineering concepts to non-thermal plasma reactors. *Plasma Sci. Technol.* **2018**, *20*, 065512. [CrossRef]

74. Mazaheri, N.; Akbarzadeh, A.H.; Madadian, E.; Lefsrud, M. Systematic review of research guidelines for numerical simulation of biomass gasification for bioenergy production. *Energy Convers. Manag.* **2019**, *183*, 671–688. [CrossRef]

75. Anis, S.; Zainal, Z.A. Tar reduction in biomass producer gas via mechanical, catalytic and thermal methods: A review. *Renew. Sustain. Energy Rev.* **2011**, *15*, 2355–2377. [CrossRef]

76. Meng, F.; Li, X.; Liang, H.; Wang, G.; Lu, L.; Liu, J. Non-thermal plasma degradation of tar in gasification syngas. *Chem. Eng. Process.—Process Intensif.* **2019**, *145*, 107656. [CrossRef]

77. Wnukowski, M.; Kordylewski, W.; Łuszkiewicz, D.; Leśniewicz, A.; Ociepa, M.; Michalski, J. Sewage Sludge-Derived Producer Gas Valorization with the Use of Atmospheric Microwave Plasma. *Waste Biomass Valorization* **2020**, *11*, 4289–4303. [CrossRef]

78. Liu, L.; Liu, Y.; Song, J.; Ahmad, S.; Liang, J.; Sun, Y. Plasma-enhanced steam reforming of different model tar compounds over Ni-based fusion catalysts. *J. Hazard. Mater.* **2019**, *377*, 24–33. [CrossRef] [PubMed]

79. Tao, K.; Ohta, N.; Liu, G.; Yoneyama, Y.; Wang, T.; Tsubaki, N. Plasma enhanced catalytic reforming of biomass tar model compound to syngas. *Fuel* **2013**, *104*, 53–57. [CrossRef]

80. Cimerman, R.; Račková, D.; Hensel, K. Tars removal by non-thermal plasma and plasma catalysis. *J. Phys. D Appl. Phys.* **2018**, *51*, 274003. [CrossRef]

81. Chun, Y.N.; Kim, S.C.; Yoshikawa, K. Decomposition of benzene as a surrogate tar in a gliding Arc plasma. *Environ. Prog. Sustain. Energy* **2013**, *32*, 837–845. [CrossRef]

82. Jamróz, P.; Kordylewski, W.; Wnukowski, M. Microwave plasma application in decomposition and steam reforming of model tar compounds. *Fuel Process. Technol.* **2018**, *169*, 1–14. [CrossRef]

83. Saleem, F.; Umer, J.; Rehman, A.; Zhang, K.; Harvey, A. Effect of Methane as an Additive in the Product Gas toward the Formation of Lower Hydrocarbons during the Decomposition of a Tar Analogue. *Energy Fuels* **2020**, *34*, 1744–1749. [CrossRef]

84. Wen, Z.; Liu, Y.; Shen, H.; Ding, N.; Li, Y.; Luo, D. Mechanism and Kinetic Study on the Degradation of Typical Biomass Tar Components (Toluene, Phenol and Naphthalene) by Ozone. *Ozone Sci. Eng.* **2021**, *43*, 78–87. [CrossRef]

85. Nair, S. Corona Plasma for Tar Removal. 2004. Available online: https://pure.tue.nl/ws/files/2272624/200412511.pdf (accessed on 13 September 2023).

86. Nair, S.A.; Nozaki, T.; Okazaki, K. Methane oxidative conversion pathways in a dielectric barrier discharge reactor—Investigation of gas phase mechanism. *Chem. Eng. J.* **2007**, *132*, 85–95. [CrossRef]

87. Pemen, A.; Nair, S.; Yan, K.; Heesch, E.J.M.; Ptasinski, K.; Drinkenburg, A. Pulsed Corona Discharges for Tar Removal from Biomass Derived Fuel Gas. *Plasmas Polym.* **2003**, *8*, 209–224. [CrossRef]

88. Wang, Y.; Liao, Z.; Mathieu, S.; Bin, F.; Tu, X. Prediction and evaluation of plasma arc reforming of naphthalene using a hybrid machine learning model. *J. Hazard. Mater.* **2021**, *404*, 123965. [CrossRef]

89. Bogaerts, A.; Eckert, M.; Mao, M.; Neyts, E. Computer modelling of the plasma chemistry and plasma-based growth mechanisms for nanostructured materials. *J. Phys. D Appl. Phys.* **2011**, *44*, 174030. [CrossRef]

90. Jiang, N.; Lu, N.; Li, J.; Wu, Y. Degradation of Benzene by Using a Silent-Packed Bed Hybrid Discharge Plasma Reactor. *Plasma Sci. Technol.* **2012**, *14*, 140–146. [CrossRef]

91. Assadi, A.A.; Bouzaza, A.; Merabet, S.; Wolbert, D. Modeling and simulation of VOCs removal by nonthermal plasma discharge with photocatalysis in a continuous reactor: Synergetic effect and mass transfer. *Chem. Eng. J.* **2014**, *258*, 119–127. [CrossRef]

92. Abdelaziz, A.A.; Seto, T.; Abdel-Salam, M.; Otani, Y. Performance of a surface dielectric barrier discharge based reactor for destruction of naphthalene in an air stream. *J. Phys. D Appl. Phys.* **2012**, *45*, 115201. [CrossRef]

93. Kang, W.; Hur, M.; Song, Y.; Hong, S. Numerical Simulation of Atmospheric-pressure Non-Equilibrium Plasmas: Status and Prospects. *Int. J. Plasma Environ. Sci. Technol.* **2013**, *7*, 104–108.

94. Dors, M.; Kurzyńska, D. Tar Removal by Nanosecond Pulsed Dielectric Barrier Discharge. *Appl. Sci.* **2020**, *10*, 991. [CrossRef]

95. Affonso Nóbrega, P.H.; Rohani, V.; Fulcheri, L. Non-thermal plasma treatment of volatile organic compounds: A predictive model based on experimental data analysis. *Chem. Eng. J.* **2019**, *364*, 37–44. [CrossRef]

96. Font Palma, C. Modelling of tar formation and evolution for biomass gasification: A review. *Appl. Energy* **2013**, *111*, 129–141. [CrossRef]

97. Fazeli, S.M.; Ravari, F.; Bozorgzadeh, H.; Sadeghzadeh Ahari, J. Kinetic model study of dry reforming of methane using cold plasma. *Phys. Chem. Res.* **2017**, *5*, 395–408. [CrossRef]

98. Gagliano, A.; Nocera, F.; Bruno, M.; Cardillo, G. Development of an Equilibrium-based Model of Gasification of Biomass by Aspen Plus. *Energy Procedia* **2017**, *111*, 1010–1019. [CrossRef]

99. Khacef, A.; Cormier, J.-M.; Pouvesle, J.; Le Van, T. Removal of Pollutants by Atmospheric Non Thermal Plasmas. *arXiv* **2008**, arXiv:0810.5432.

100. Mizuno, A. Industrial applications of atmospheric non-thermal plasma in environmental remediation. *Plasma Phys. Control. Fusion* **2007**, *49*, A1–A15. [CrossRef]

101. Kacprzyk, R.; Mista, W.; Czapka, T. Atmospheric pressure cold plasma reactor with back discharges and parallel gas flow. *Int. J. Plasma Environ. Sci. Technol.* **2011**, *5*, 58–61.

102. Abdelaziz, A.A.; Ishijima, T.; Seto, T. Humidity effects on surface dielectric barrier discharge for gaseous naphthalene decomposition. *Phys. Plasmas* **2018**, *25*, 043512. [CrossRef]

103. Delikonstantis, E.; Scapinello, M.; Stefanidis, G.D. Process Modeling and Evaluation of Plasma-Assisted Ethylene Production from Methane. *Processes* **2019**, *7*, 68. [CrossRef]

104. Li, Q.; Wang, Q.; Tsuboi, Y.; Zhang, J.; Liu, J. Steam reforming of tar studied in bench-scale experiments and pilot-scale tests with simulations. *Fuel* **2021**, *290*, 120028. [CrossRef]

105. Arshad, M.Y.; Saeed, M.A.; Tahir, M.W.; Pawlak-Kruczek, H.; Ahmad, A.S.; Niedzwiecki, L. Advancing Sustainable Decomposition of Biomass Tar Model Compound: Machine Learning, Kinetic Modeling, and Experimental Investigation in a Non-Thermal Plasma Dielectric Barrier Discharge Reactor. *Energies* **2023**, *16*, 5835. [CrossRef]

106. Wang, T.C.; Lu, N.; Li, J.; Wu, Y. Degradation of pentachlorophenol in soil by pulsed corona discharge plasma. *J. Hazard. Mater.* **2010**, *180*, 436–441. [CrossRef]

107. Zhang, X.; Chen, W.W.; Zhu, J.; Feng, W.; Yan, K. Aerosol Formation and Decomposition of Benzene Derivatives by AC/DC Streamer Corona Discharge. *Int. J. Plasma Environ. Sci. Technol.* **2010**, *4*, 130–134.

108. Anderson, G.K.; Snyder, H.; Coogan, J. Oxidation of Styrene in a Silent Discharge Plasma. *Plasma Chem. Plasma Process.* **1999**, *19*, 131–151. [CrossRef]

109. Anis, S.; Zainal, Z.A. Study on kinetic model of microwave thermocatalytic treatment of biomass tar model compound. *Bioresour. Technol.* **2014**, *151*, 183–190. [CrossRef]

110. Karatum, O.; Deshusses, M.A. A comparative study of dilute VOCs treatment in a non-thermal plasma reactor. *Chem. Eng. J.* **2016**, *294*, 308–315. [CrossRef]

111. Mei, D.; Tu, X. Conversion of CO2 in a cylindrical dielectric barrier discharge reactor: Effects of plasma processing parameters and reactor design. *J. CO2 Util.* **2017**, *19*, 68–78. [CrossRef]

112. Wang, C.; Zhu, L.; Zhao, F.; Xu, D. The chemistry of gaseous benzene degradation using non-thermal plasma. *Environ. Sci. Pollut. Res.* **2021**, *28*, 1565–1573. [CrossRef]

113. Abdelaziz, A.A.; Seto, T.; Abdel-Salam, M.; Otani, Y. Influence of N2/O2 Mixtures on Decomposition of Naphthalene in Surface Dielectric Barrier Discharge Based Reactor. *Plasma Chem. Plasma Process.* **2014**, *34*, 1371–1385. [CrossRef]

114. Bityurin, V.A.; Filimonova, E.A.; Naidis, G.V. Simulation of Naphthalene Conversion in Biogas Initiated by Pulsed Corona Discharges. *IEEE Trans. Plasma Sci.* **2009**, *37*, 911–919. [CrossRef]

115. Lorcet, H.; Guenadou, D.; Latge, C.; Brothier, M.; Mariaux, G.; Vardelle, A. Kinetics modeling of biomass gasification under thermal plasma conditions. Application to a refractory species: The methane. In *International Symposium on Plasma Chemistry, Germany*; International Union of Pure and Applied Chemistry: Research Triangle Park, NC, USA, 2022.

116. Yan, K.; van Heesch, E.J.M.; Pemen, A.J.M.; Huijbrechts, P.A.H.J. From Chemical Kinetics to Streamer Corona Reactor and Voltage Pulse Generator. *Plasma Chem. Plasma Process.* **2001**, *21*, 107–137. [CrossRef]

117. Nair, S.A.; Yan, K.; Pemen, A.J.M.; van Heesch, E.J.M.; Ptasinski, K.J.; Drinkenburg, A.A.H. Tar Removal from Biomass-Derived Fuel Gas by Pulsed Corona Discharges. A Chemical Kinetic Study. *Ind. Eng. Chem. Res.* **2004**, *43*, 1649–1658. [CrossRef]

118. Filimonova, E.A.; Amirov, R.H.; Kim, H.T.; Park, I.H. Comparative modelling of NOx and SO2 removal from pollutant gases using pulsed-corona and silent discharges. *J. Phys. D Appl. Phys.* **2000**, *33*, 1716–1727. [CrossRef]

119. Blin-Simiand, N.; Jorand, F.; Magne, L.; Pasquiers, S.; Postel, C.; Vacher, J.R. Plasma Reactivity and Plasma-Surface Interactions During Treatment of Toluene by a Dielectric Barrier Discharge. *Plasma Chem. Plasma Process.* **2008**, *28*, 429–466. [CrossRef]

120. Mariana, F.M.; Antonio, M.C.; Raúl, V.A.; Régulo, L.C.; Samuel, B.D.; Rosendo, P.E.; Arturo, M.C.; Bethsabet, J.S. NOx Chemical Reduction in a Cylindrical DBD Reactor: Theoretical and Experimental Analysis. *Conf. Fr. Electrost.* **2008**, *3*, 98.

121. Ratkiewicz, A.; Truong, T. A canonical form of the complex reaction mechanism. *Energy* **2012**, *43*, 64–72. [CrossRef]

122. Nair, S.A.; Yan, K.; Pemen, A.J.M.; van Heesch, E.J.M.; Ptasinski, K.J.; Drinkenburg, A.A.H. Tar Removal from Biomass Derived Fuel Gas by Pulsed Corona Discharges: Chemical Kinetic Study II. *Ind. Eng. Chem. Res.* **2005**, *44*, 1734–1741. [CrossRef]

123. Kraus, M.; Egli, W.; Haffner, K.; Eliasson, B.; Kogelschatz, U.; Wokaun, A. Investigation of mechanistic aspects of the catalytic CO2 reforming of methane in a dielectric-barrier discharge using optical emission spectroscopy and kinetic modeling. *Phys. Chem. Chem. Phys.* **2002**, *4*, 668–675. [CrossRef]

124. Bityurin, V.A.; Filimonova, E.A.; Kerst, R.A.B.P.; Naidis, G.V.; Pemen, A.J.M. The modeling of tar removal from biogas stimulated by a pulse corona discharge. *Vacuum* **2006**, *2*, N2.

125. Heesch, B.E.J.M.V.; Pemen, G.U.A.J.M.; Keping, Y.; Paasen, S.V.B.V.; Ptasinski, K.J.; Huijbrechts, P.A.H.J. Pulsed corona tar cracker. *IEEE Trans. Plasma Sci.* **2000**, *28*, 1571–1575. [CrossRef]

126. Kim, H.-H.; Ogata, A.; Futamura, S. Atmospheric plasma-driven catalysis for the low temperature decomposition of dilute aromatic compounds. *J. Phys. D Appl. Phys.* **2005**, *38*, 1292–1300. [CrossRef]

127. Jiang, N.; Lu, N.; Shang, K.; Li, J.; Wu, Y. Effects of electrode geometry on the performance of dielectric barrier/packed-bed discharge plasmas in benzene degradation. *J. Hazard. Mater.* **2013**, *262*, 387–393. [CrossRef] [PubMed]

128. Lotfi, S.; Ma, W.; Austin, K.; Kumar, A. A wet packed-bed scrubber for removing tar from biomass producer gas. *Fuel Process. Technol.* **2019**, *193*, 197–203. [CrossRef]

129. Materazzi, M.; Lettieri, P.; Mazzei, L.; Taylor, R.; Chapman, C. Reforming of tars and organic sulphur compounds in a plasma-assisted process for waste gasification. *Fuel Process. Technol.* **2015**, *137*, 259–268. [CrossRef]